Title

Metabolome Changes during In Vivo Red Cell Aging Reveal Disruption of Key Metabolic Pathways

Journal

iScience, 23(10)

ISSN

2589-0042

Authors

Jamshidi, Neema
Xu, Xiuling
von Löhneysen, Katharina
et al.

Publication Date

2020-10-01

DOI

10.1016/j.isci.2020.101630

Peer reviewed

iScience

CellPress
OPEN ACCESS

Article

Metabolome Changes during *In Vivo* Red Cell Aging Reveal Disruption of Key Metabolic Pathways

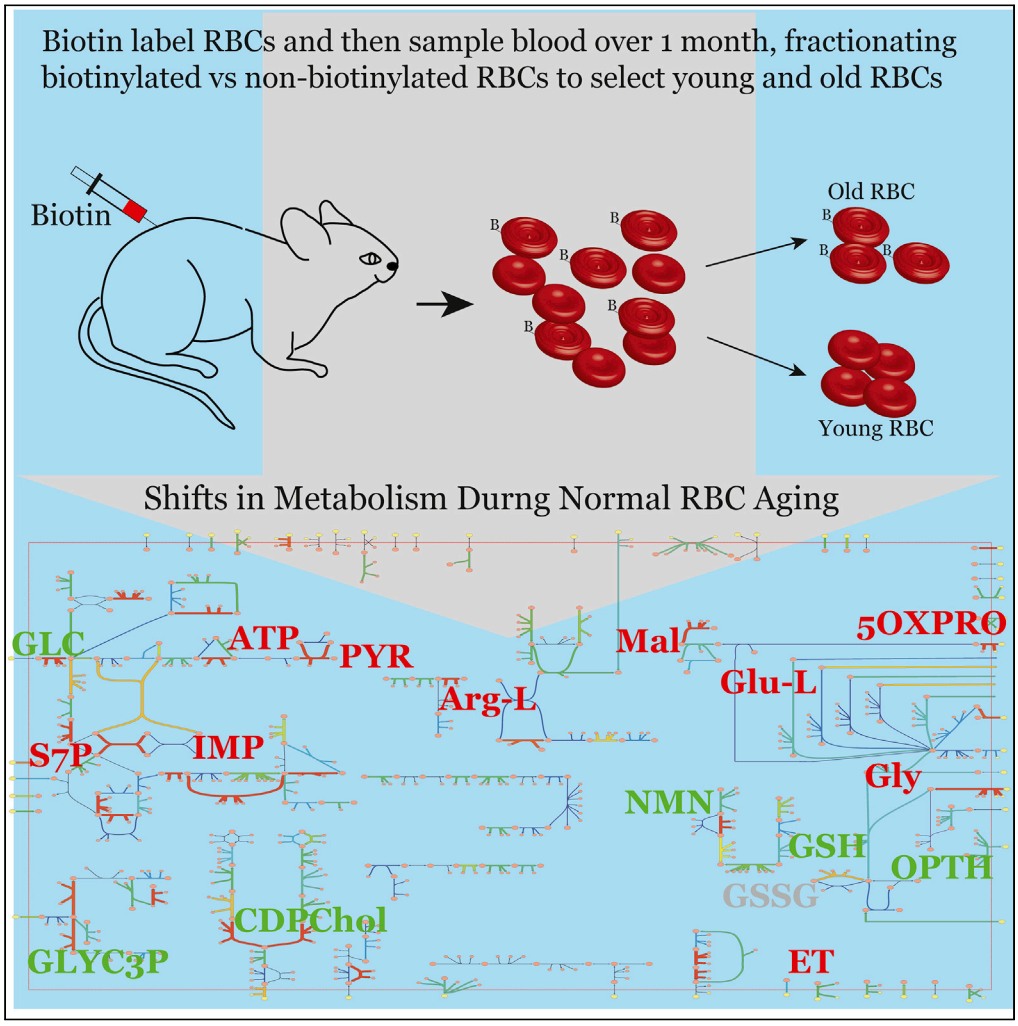

Neema Jamshidi, Xiuling Xu, Katharina von Löhneysen, ..., Edward D. Karoly, Mike Scott, Jeffrey S. Friedman

friedmanbioventure@icloud.com

HIGHLIGHTS

Altered glycolytic, amino acid, and fatty acid metabolism occurs in normal RBC aging

GSH pools are maintained in spite of age-dependent shifts in enzyme synthesis

Changes in choline and GPC suggest alterations in membrane lipid metabolism

Ophthalmate, GPC, and ergothioneine are candidate metabolic clocks for RBC aging

Jamshidi et al., iScience *23*, 101630
October 23, 2020
https://doi.org/10.1016/j.isci.2020.101630

iScience

CellPress
OPEN ACCESS

Article

Metabolome Changes during *In Vivo* Red Cell Aging Reveal Disruption of Key Metabolic Pathways

Neema Jamshidi,[5,6] Xiuling Xu,[2] Katharina von Löhneysen,[8] Katrin Soldau,[3] Rob P. Mohney,[4] Edward D. Karoly,[4] Mike Scott,[7] and Jeffrey S. Friedman[1,9,10,*]

SUMMARY

Understanding the mechanisms for cellular aging is a fundamental question in biology. Normal red blood cells (RBCs) survive for approximately 100 days, and their survival is likely limited by functional decline secondary to cumulative damage to cell constituents, which may be reflected in altered metabolic capabilities. To investigate metabolic changes during *in vivo* RBC aging, labeled cell populations were purified at intervals and assessed for abundance of metabolic intermediates using mass spectrometry. A total of 167 metabolites were profiled and quantified from cell populations of defined ages. Older RBCs maintained ATP and redox charge states at the cost of altered activity of enzymatic pathways. Time-dependent changes were identified in metabolites related to maintenance of the redox state and membrane structure. These findings illuminate the differential metabolic pathway usage associated with normal cellular aging and identify potential biomarkers to determine average RBC age and rates of RBC turnover from a single blood sample.

INTRODUCTION

Erythrocytes are the most abundant cells in humans (approximately 25 trillion circulating cells in the "average" adult male) with an average lifespan of approximately 100 days and interactions with all cellular tissue in the body, either directly or via diffusion or active transport mechanisms, and they are highly dynamic. Although the principle function of these cells is to facilitate oxygen transport and carbon dioxide elimination, their ability to metabolize sugars, amino acids, and fatty acids reflects a set of biochemical capabilities comparable with small organisms. Understanding the dynamic changes in metabolic function and capabilities of erythrocytes represents a fundamental question in biology and mammalian physiology as well as a question of great potential practical import to biomedical sciences and medicine.

Mature red blood cells (RBCs) cannot synthesize new proteins and have little ability to repair damage. Limitations on RBC survival are thus likely due to accumulation of damage to critical cellular components including enzymes involved in glucose and redox metabolism, structural proteins, and hemoglobin, as defects in these targets accelerate RBC turnover and are common causes of hereditary anemia. Several mechanisms have been proposed to explain the normal removal of senescent RBC or the premature removal of damaged RBC in hemolytic disorders. Studies separating young versus old RBC based upon density reported that changes in band 3 protein (Low et al., 1985) such as oxidation (Beppu et al., 1990), or the appearance of a "senescent antigen" (Kay et al., 1991) facilitated antibody binding to aged cells, hastening their removal. Changes in the content or composition of sugar residues of RBC membrane glycoproteins have been described during cell aging and have been associated with differential binding to phagocytic cells (Vaysse et al., 1986). A change in membrane phospholipid asymmetry (abnormal exposure of phosphatidyl serine [PS] on the outer surface) has been demonstrated in sickle cell anemia (Kuypers et al., 1996) and in response to a growing list of exogenous shocks (glucose deprivation, oxidative stress, osmotic shock, ceramide, and a variety of drugs and toxins) collectively described as "eryptosis," the RBC equivalent of apoptosis (Foller et al., 2008; Lang et al., 2005).

However, the series of events in normal RBC aging leading to RBC destruction remains incompletely defined. It is presumed that progressive metabolic defects ultimately affect energy-dependent

[1]Friedman Bioventure, Inc, San Diego, CA, USA

[2]The Scripps Research Institute, Department of Molecular and Experimental Medicine, La Jolla, CA, USA

[3]University of California, San Diego, Department of Pathology, La Jolla, CA, USA

[4]Metabolon, Inc, Durham, NC, USA

[5]University of California, San Diego, Institute of Engineering in Medicine, La Jolla, CA, USA

[6]University of California, Los Angeles, Department of Radiological Sciences, Los Angeles, CA, USA

[7]San Diego Mesa College, Chemistry Department, San Diego, CA, USA

[8]Mitokinin, Inc, San Francisco, CA, USA

[9]DTx Pharma, Inc, San Diego, CA, USA

[10]Lead Contact

*Correspondence: friedmanbioventure@icloud.com

https://doi.org/10.1016/j.isci.2020.101630

maintenance functions of the RBC (van Wijk and van Solinge, 2005) such as sustaining the electrolyte gradient across the red cell membrane; maintenance of hemoglobin in an active, reduced state; protection of enzymes and membrane proteins from oxidative damage, -in part through synthesis and regeneration of reduced glutathione; maintenance of phospholipid asymmetry in the membrane and provision of the ATP required for the first steps of glycolysis. Such metabolic changes in the RBC cytosol must be translated into changes in physical properties of the cell that can be recognized from the outside by phagocytic cells, as the terminal event in RBC lifespan occurs when macrophages recognize and engulf the compromised cell.

Here we present the results of untargeted metabolomic analysis of normal RBC isolated at early, mid, and late time points during *in vivo* aging in mice. Metabolite profiles demonstrate early changes associated with the reticulocyte to mature RBC transition, as well as changes in glucose utilization and glutathione metabolism with cell aging, identifying several metabolites that may be useful as surrogate markers of RBC age. Critically, we identify several changes impacting cellular response to oxidative damage, including a decline in the concentration of ergothioneine, a xenobiotic antioxidant compound derived from the diet, and accumulation of the glutathione analog ophthalmate, a potentially toxic product that may inhibit RBC glutathione utilization. Although the link between cytosolic metabolic changes and the appearance of cell surface signals leading to recognition by phagocytic cells remains elusive, we observed a dramatic increase in glycerophosphocholine (GPC, a precursor or breakdown product of membrane phospholipid) and a steep decline in sialic acid (n-acetyl neuraminate) in RBC as a function of cell age. Changes in sialic acid content of RBC membrane (Aminoff et al., 1977) and immune recognition of GPC-like determinants on RBC membranes (Arnold and Haughton, 1992; Mercolino et al., 1986) have previously been implicated in RBC turnover. These results support a model in which metabolic changes impair the ability of RBC to utilize energy in the form of glucose, reduce their capacity to counteract oxidative damage, and potentially alter membrane surface characteristics with increasing age *in vivo*.

RESULTS

Red Cell Survival Kinetics in Wild-Type Mice

In order to study biochemical changes as a function of RBC age, we coupled *in vivo* surface biotin labeling, a method that is now commonly used to follow RBC survival (Cohen et al., 2008; Friedman et al., 2001; Hoffmann-Fezer et al., 1991), with cell separation utilizing magnetic beads in order to isolate RBC of defined age for analysis. Figure 1A shows a representative RBC survival curve using male C57Bl6/J mice following *in vivo* biotin labeling. Normal murine RBC were removed at a rate approximating a linear function of cell age with a half-life of about 22 days and a maximal lifespan approaching 60 days, with no evidence for significant random destruction of RBC. Following biotin labeling, RBC were separated from unlabeled cells using streptavidin magnetic beads as show in Figure 1B. Bead separation consistently yielded >90% biotinylated RBC in the column-bound fraction (average % biotin positive 96.4%), and yielded unlabeled RBC in the column flow-through of slightly lower purity (average % biotin negative 87%; see Table S1 for detailed purification data). The biotin positive (+) fraction contains all cells that were present at the time of labeling, and therefore must be at least as old as the number of days elapsed since labeling, whereas the biotin negative fraction (–) contains all cells younger than or equal to the number of days since labeling.

Metabolite Changes in Young versus Old RBCs

Biotin (+) and biotin (–) fractions were collected 8, 15, and 35 days following labeling (see schematic, Figure 1C) for comparative analysis of metabolite concentrations determined using a multiplatform mass spectrometry approach (Evans et al., 2009). A total of 167 known biochemical metabolites were detected in RBC extracts collected at 8, 15, and 35 days after labeling, using 5 or 6 biologic replicates for each time point. Comparisons between biotin (+) [old] and biotin (–) [young] cells were performed for each time point, and the change in each metabolite was assessed over the entire time course. Principle component analysis (Figure 2A) shows a tight grouping of replicate samples and provides a graphic depiction of how similar or distant overall metabolite profiles are among samples analyzed. Figure 2B presents a pie chart dividing up identified metabolites by compound class, with lipids and amino acids representing the two largest classes. Figure 2C uses the same classification of compounds to organize a heatmap of changes in concentration of individual metabolites. A complete listing of all metabolites identified is presented in Table S2 along with changes in metabolite relative concentration as a function of RBC age. Multiple metabolites showed statistically significant changes in their relative concentration as a function of RBC age (Table 1). In the most extreme comparison of RBC 8 days or younger against RBC 35 days or older, 108 of 167 metabolites were significantly different ($p \leq 0.05$, Welch's two-sample t test). Of these 108

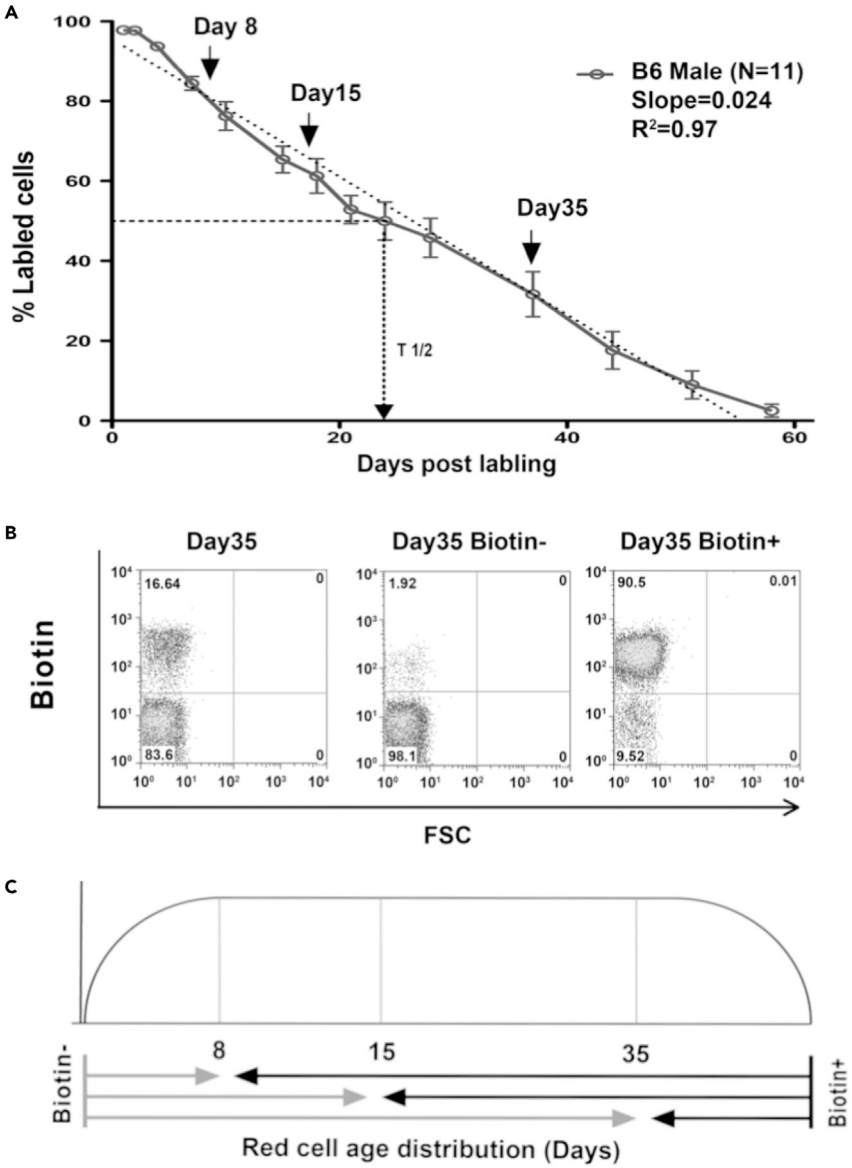

Figure 1. Red Cell Survival, Cell Separation, and Experimental Design

(A) Results of a representative RBC survival experiment in male C57Bl6/J mice using the *in vivo* biotin labeling approach. Care was taken to collect very small volumes of blood (1–5 μL) at each time point to avoid skewing the results with random cell loss due to phlebotomy. Under these conditions, RBC half-life is approximately 23 days, with maximal RBC lifespan 58 days. The survival curve closely approximates a linear function, with the loss of ~2.4% of RBC each day. Arrows indicate the timing of harvest for separate cohorts used for metabolomic analyses. Data are represented as +/− SEM.

(B) Results of a representative magnetic bead separation of RBC at the 35-day time point. Unfractionated cells (left), biotin(−), and biotin(+) are shown. Bead separations routinely yielded high-purity populations in both biotin(−) and biotin(+) fractions. Complete purification results are presented in Table S1.

(C) Schematic view of the age distribution of the RBC populations used in metabolomic analyses. Without evidence for significant random destruction of RBCs, the best approximation of age distribution is a conveyor belt, where RBCs enter the circulation and remain until removal at or near the maximal lifespan.

metabolites, 89 were found to be decreased, whereas 19 were found to be elevated in older RBC. In the least disparate comparison of RBC 15 days or older versus RBC 8 days or older, 25 of 167 metabolites were significantly different. Of these 25 metabolites, 21 were decreased in older cells, whereas 4 were increased. For all comparisons, the number of metabolites that declined with increasing RBC age exceeded the number of metabolites that increased with age. Many of the metabolites that drop reflect

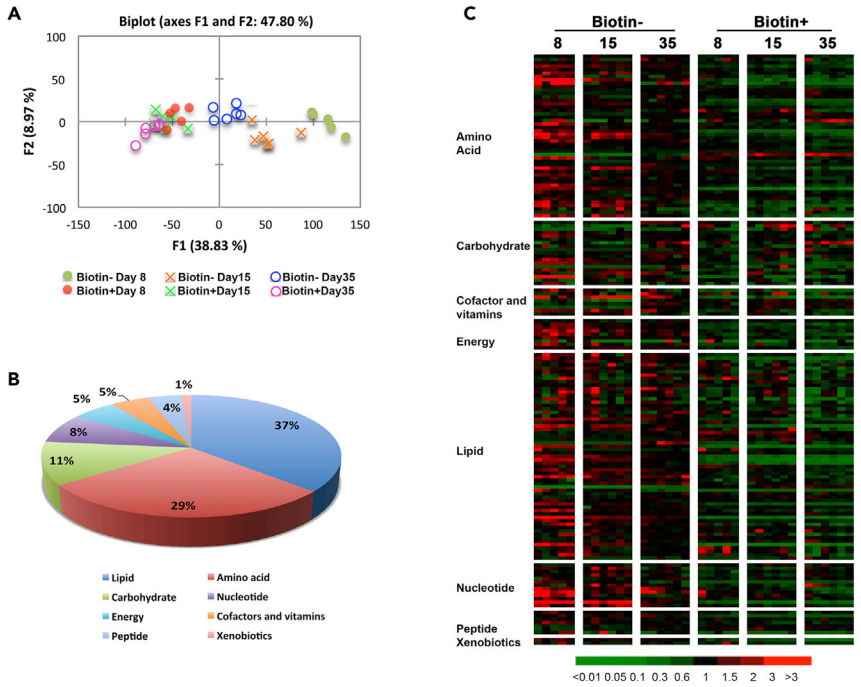

Figure 2. Overview of Metabolomic Analysis

(A) Principal component analysis was used as an overall method to assess data quality and compare sample groups. At each time point, biologic replicate samples cluster together by age (biotin + or biotin -). Biotin(+) samples at different time points are more similar to each other than biotin(−) samples, with cells ≤8 days being the most divergent.

(B) Distribution of metabolites according to compound class, with lipids and amino acids representing two-thirds of all compounds identified.

(C) Heatmap summarizing all metabolite data by compound class over the time course of this study. The predominant pattern of metabolite change across all compound classes is a decline with increasing RBC age. Data presented are from five biologic replicates at day 8 and six replicates for days 15 and 35.

changes that occur at the reticulocyte to mature RBC transition in the first few days of RBC lifespan, for instance, loss of mitochondria (multiple carnitines decline) and cessation of protein synthesis (multiple amino acids decline). Representative examples of metabolite profiles including these common patterns are shown in Figure S1.

Relative Mass Action Ratios

Among the 167 compounds identified are several not previously recognized as metabolic intermediates in RBC, although in many cases synthetic routes for their production utilize well-established RBC pathways. Calculation of relative Mass Action Ratios (rMAR) (see Methods and Supporting Information) highlight the changes in the thermodynamic driving potential for the biochemical reaction network. In the context of intracellular metabolomic profiling of *in vivo* RBC over time, the increased rMARs can be used to identify age-dependent rate limitations of enzymes, or "age-limiting" enzymes. Figure S2 provides a color-coded rMAR map (day 8 versus day 35) of the metabolites onto an integrated flux balanced RBC metabolic model map derived from prior experimental and modeling studies that incorporated proteomic, enzymatic, and metabolomic data (Bordbar et al., 2011). Figure 3 highlights three different areas of metabolism within the network that have shifts in metabolites that may be attributable to age-limiting enzymes, drawing attention to sugar metabolism (for maintenance of high energy phosphate pools), amino acid/glutathione metabolism (for maintenance of redox states), and fatty acid metabolism (for maintenance of cell membrane structure and biochemical composition).

Glucose Metabolism

Glucose concentration was increased, whereas levels of both glucose 6-P and fructose 6-P were decreased in older RBCs (Figure 4A), indicating a reduced capacity to utilize glucose. Additional downstream

Comparison	Number of Metabolites ($p < 0.05$)
Welch's Two-Sample t test	
Biotin (+) day 35 vs biotin (–) day 8	108 (19 up, 89 down)
Biotin (–) day 15 vs biotin (–) day 8	54 (12 up, 42 down)
Biotin (–) day 35 vs biotin (–) day 8	73 (22 up, 51 down)
Biotin (–) day 35 vs biotin (–) day 15	61 (27 up, 34 down)
Biotin (+) day 15 vs biotin (+) day 8	25 (4 up, 21 down)
Biotin (+) day 35 vs biotin (+) day 8	44 (7 up, 37 down)
Biotin (+) day 35 vs biotin (+) day 15	31 (5 up, 26 down)
Paired t Test	
Biotin (+) day 8 vs biotin (–) day 8	95 (20 up, 75 down)
Biotin (+) day 15 vs biotin (–) day 15	92 (26 up, 66 down)
Biotin (+) day 35 vs biotin (–) day 35	88 (8 up, 80 down)

Table 1. Summary of Statistical Comparison of RBC Metabolites as a Function of Cell Age

metabolites in the glycolytic (pyruvate) and pentose phosphate (sedoheptulose 7-P) pathways were also found to be lower in older RBCs. We measured hexokinase activity in young versus old RBC preparations in order to determine whether changes in enzymatic activity correlated with the observed change in metabolite pattern (Figure 4B). Hexokinase activity was significantly lower in older RBC when comparing young versus old RBC fractions assayed at days 8, 15, and 35 after biotin labeling, in agreement with prior studies that reported lower activity in older cells (Beutler and Hartman, 1985; Thorburn and Beutler, 1991; Zimran et al., 1988). However, the bulk of this decline appears to occur relatively early in RBC lifespan, with modest incremental decline in activity at increasing cell age. This suggests that impaired glucose utilization in older RBC may involve both a cell age-related decline in hexokinase activity and an additional factor, such as a decline in ATP levels (ATP is the high energy phosphate donor in the hexokinase reaction) with increasing cell age. In order to test this possibility, we measured ATP levels in young versus old RBC (Figure 4C) and found that older RBC consistently had lower ATP concentrations. However, similar to results with hexokinase activity, much of the decline in ATP concentration occurs early in RBC lifespan, with no indication that the drop in ATP levels is progressive with increasing cell age at the time points tested. We also measured G6PD activity as a function of RBC age, again finding decreasing activity in older cells (Figure 4). For G6PD activity, there appears to be a more gradual, but progressive, loss over time.

Glutathione Synthesis and Utilization

We next turned our attention to metabolic pathways that protect against oxidative damage. From results of earlier publications that attempted to separate young and old RBCs (Clark and Shohet, 1985; Rettig et al., 1999), we expected to find a decline in reduced glutathione (GSH) and an increase in oxidized glutathione (GSSG) with increasing RBC age. A more recent study from our own laboratory using a redox-sensitive green fluorescent protein sensor in RBC also demonstrated a shift to a more oxidized redox potential with increasing RBC age (Xu et al., 2011). However, as shown in Figure 5A, we found that GSH showed a

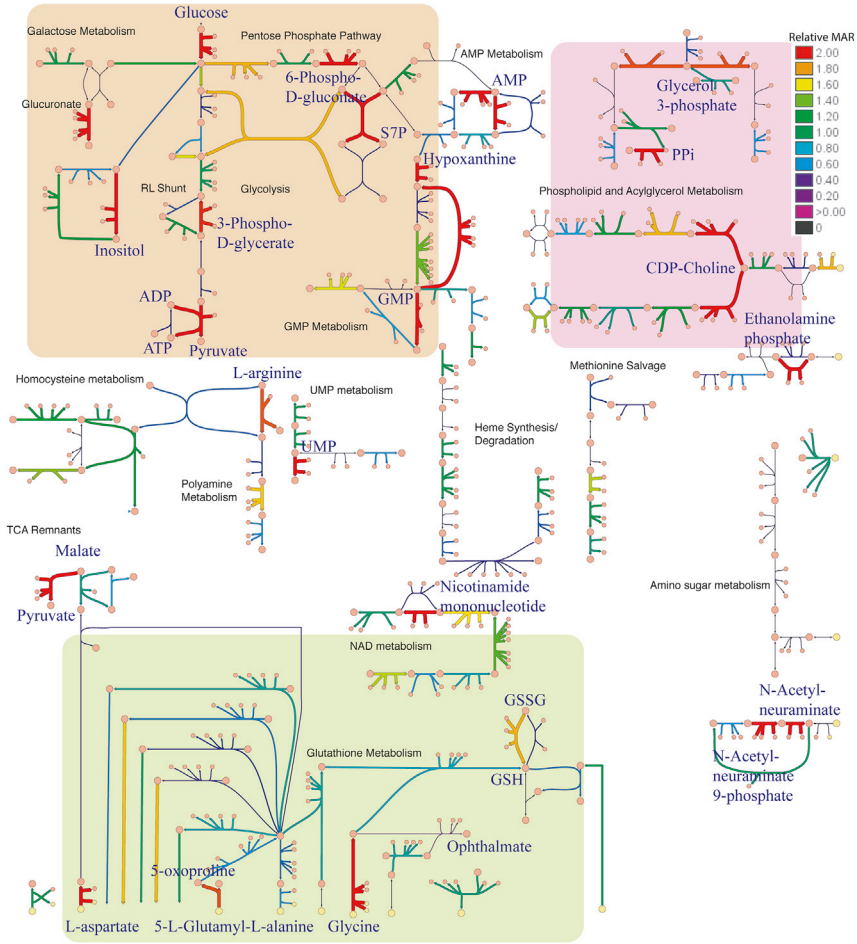

Figure 3. Changes in Metabolite Production and Consumption in the Red Cell Metabolic Network

RBC metabolic map highlighting systemic metabolic shifts during cellular senescence. Reaction arrow thickness and color coding correspond to rMAR magnitude changes (day 8 versus day 35; all ratios greater than two are shaded red and black is 0). Three subsystems of metabolism are highlighted, sugar metabolism for energy (orange), amino acid/glutathione metabolism for redox homeostasis (green), and fatty acid metabolism for membrane/structural maintenance (pink). High rMAR reactions (thick, red arrows, rMAR ≥ 2) reflect bottlenecks with accumulation of enzyme substrates, identifying potential "age-limited" enzymes (the corresponding metabolites are highlighted in blue text). Metabolic subsystems are labeled in black font text. See Figure S2 for a high-resolution, detailed labeled version.

small increase, whereas GSSG was not significantly different when comparing old and young RBCs, with no consistent trajectory for these biochemicals as a function of cell age (data not shown). Evaluation of several precursors for glutathione synthesis including glycine and glutamate revealed significantly lower concentrations in older RBC (Figure 5B), indicating that, although GSH level does not drop with age, GSH synthesis is likely to be reduced in older RBC. Cysteine, the rate-limiting reagent for glutathione synthesis, was not detected in any RBC extracts, indicating scarcity but providing no direct information on changes in concentration with RBC aging. However, additional cysteine and glutathione-related metabolites were detected, including cysteinyl-glycine and cysteine-glutathione disulfide. These metabolites were significantly lower in old RBC providing indirect evidence for cysteine limitation in old versus young cells. Further evidence for limited cysteine comes from detection of ophthalmate, a GSH analog, at ~40-fold higher levels in the oldest RBC. Ophthalmate, which is synthesized by glutathione synthetase (GS), is structurally similar to glutathione with the cysteine group replaced by 2-aminobutyrate (Kombu et al., 2009; Soga et al., 2006).

We reasoned that decreased GSH synthesis could be balanced by decreased GSH utilization in older RBCs, thereby maintaining GSH levels. Therefore, we investigated whether the activity of GSH utilizing and regenerating enzymes was altered with increasing cell age. Figures 6A–6D show comparisons of enzymatic

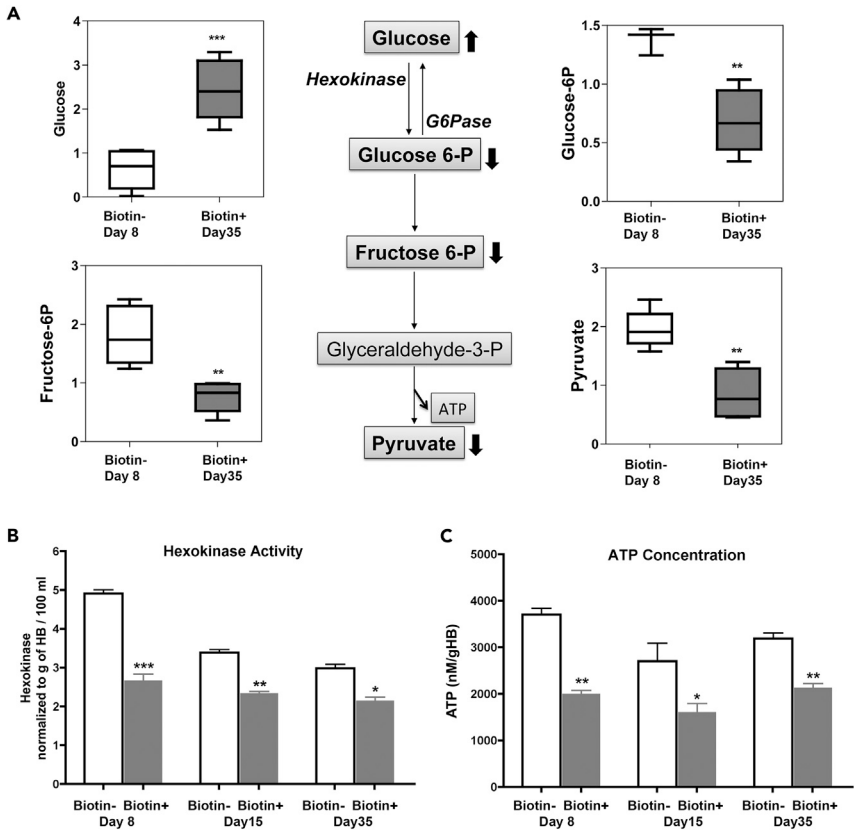

Figure 4. Change in Metabolites in Glycolytic Pathway

(A) Schematic of the glycolytic pathway. Metabolites with statistically significant changes in concentration are accompanied by a block arrow showing the direction of change over the course of RBC aging. Box plots for each metabolite are shown comparing metabolite concentration in cells ≤8 days versus cells ≥35 days. In addition to changes in the glycolytic pathway, we also found reduced concentration of sedoheptulose 7-P, a downstream metabolite in the pentose phosphate pathway.

(B) Hexokinase activity was compared in RBC hemolysates prepared from cells of the indicated ages. Hexokinase activity is highest in the youngest RBC fraction and shows a modest progressive decline in activity with increasing RBC age.

(C) ATP levels were determined in the same cell fractions as used above. ATP concentration is consistently higher in the young cell fractions, without evidence of a further decline as a function of RBC age.

(Data presented in (A) were derived from five or six biologic replicates; data in (B and C) were derived from four biologic replicates, summarized as mean values +/− SEM. Asterisks indicate significance at * <0.05, ** <0.01, and *** <0.001, respectively, assessed with paired t tests).

activity of glutathione-S-transferase (GST), glutaredoxin (GRedoxin), glutathione peroxidase (GPx), and glutathione reductase (GReductase) in hemolysates prepared from RBCs of defined age. As demonstrated earlier with hexokinase and G6PD activities, there was a reproducible, age-dependent decline in the activity of each enzyme (most dramatically for GST) with the exception of GPx. The decline in activity of both GST and GRedoxin appear to be progressive with age, whereas GReductase activity changes little after a drop early in RBC lifespan.

In addition to the age-related reduction in activity of GST and GRedoxin shown above, the accumulation of ophthalmate over time might also have an impact on GSH utilization. In order to assess this, we repeated enzymatic assays using normal (unfractionated by age) RBC lysates in the presence of increasing amounts of ophthalmate (Figure 6G). We found that GRedoxin activity was reduced in the presence of increasing concentrations of ophthalmate and GST activity was reduced at the highest concentration tested, indicating that ophthalmate acts as an inhibitor, presumably competitive based upon structural similarity to GSH. GPx activity was unaffected, whereas we observed an unexplained but reproducible increase in GReductase activity in the presence of ophthalmate.

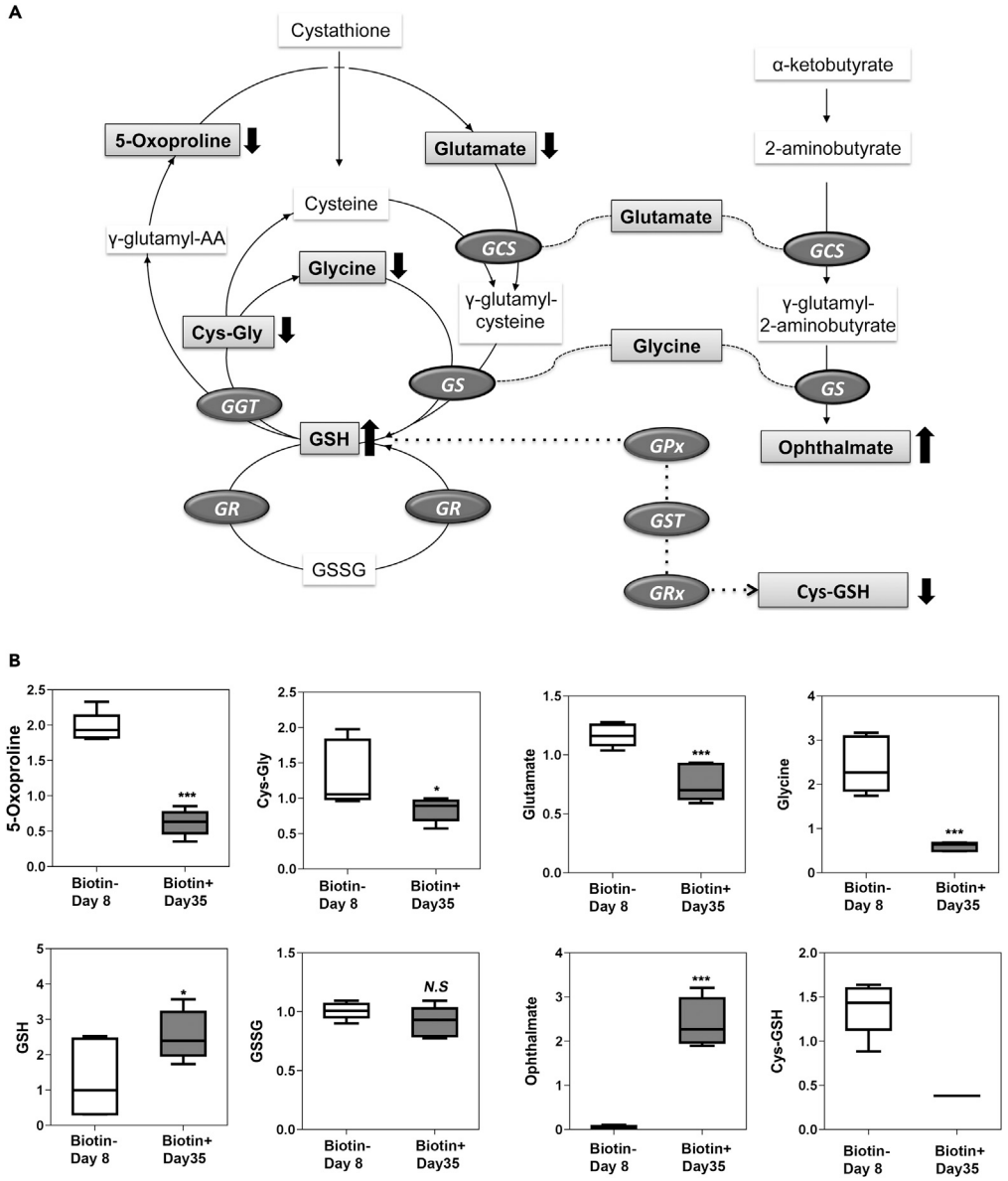

Figure 5. Glutathione Synthesis and Utilization as a Function of RBC Age

(A) Schematic metabolic pathways including GSH synthesis, utilization, and regeneration are depicted along with a parallel pathway for ophthalmate synthesis indicating common precursors. Several intermediates in the glutathione synthetic pathway are present at significantly lower concentration in old RBC (bold downward arrows). Despite reduced precursor concentrations, GSH level was modestly increased in older cells (*$p \leq 0.05$) and GSSG level did not change with RBC age.

(B) Box plots comparing concentrations of specific metabolites from young RBCs ($\leq$8 days) and old RBCs ($\geq$35 days). The combination of increased GSH level, unchanged GSSG level, and reduced cys-GSH level is consistent with reduced GSH cycling in older cells. The increased concentration of ophthalmate indicates that the GSH synthetic machinery is intact but that cysteine is lacking for GSH synthesis.

(Data were derived from five or six biologic replicates, summarized as mean values +/− SEM. Asterisks indicate significance at * <0.05 and *** <0.001, respectively, assessed with paired t tests and Welch's two-sample t test for non-paired sample groups).

We next asked whether the concentration of ophthalmate in older RBCs was high enough to mediate inhibition *in vivo*. Because the initial untargeted metabolomic analysis was designed to provide relative, but not absolute, metabolite concentrations, we devised a quantitative method for ophthalmate

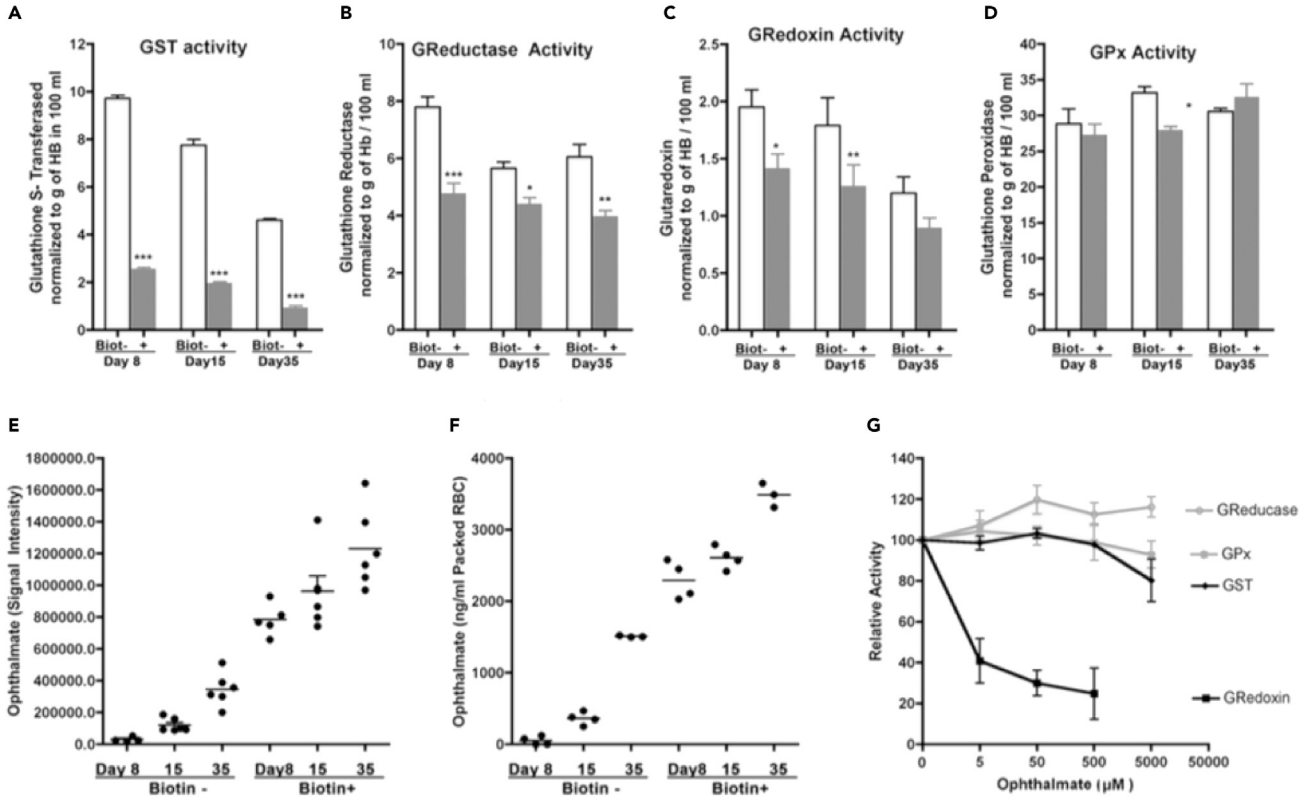

Figure 6. Activity of GSH-Utilizing Enzymes, Ophthalmate Concentration, and Effect of Ophthalmate on Activity

(A–D): Enzymatic activity of (A) glutathione-S-transferase (GST), (B) glutathione reductase (GReductase), (C) glutaredoxin (GRedoxin), and (D) glutathione peroxidase (GPx) was compared in RBC hemolysates prepared from young versus old RBCs harvested 8, 15, or 35 days after biotin labeling. GRedoxin and GST both had significantly reduced activity in the old RBC fractions and showed a progressive loss of activity with increasing RBC age. GReductase activity was higher in young RBCs, without progressive loss of activity with increasing RBC age. In contrast, GPx activity was preserved with RBC aging, and there was no differential activity observed when comparing young versus old RBCs.

(E) Relative ophthalmate concentration data from untargeted analysis (showing five or six biologic replicates for each time point).

(F) Absolute ophthalmate concentration derived from independent experiment with targeted metabolomic approach using deuterated ophthalmate spike (showing three or four biologic replicates per time point). The rise in ophthalmate concentration with increasing RBC age was confirmed in this independent experiment.

(G) Enzymatic activity assays (as in A–D) were repeated using normal murine RBC hemolysate in the presence of increasing concentrations of ophthalmate. GRedoxin shows a dose-dependent reduction in activity with increasing concentrations of ophthalmate.

(Inhibition data are derived from testing hemolysates from two animals, using triplicate wells for each sample at each concentration tested. Results are representative of two independent experiments, summarized as mean values +/− SEM. Asterisks indicate significance at * <0.05, ** <0.01, and *** <0.001, respectively, assessed with paired t tests and Welch's two-sample t test for non-paired sample groups).

measurement using a stable isotope-labeled (deuterated) ophthalmate standard. A new RBC survival study was performed with samples collected at 8, 15, and 35 days following labeling. As shown in Figures 6E (original relative data) and 6F (new replicate data with quantification), these results confirm that ophthalmate increases dramatically with RBC aging. In RBC 8 days or younger, ophthalmate concentrations were too low to reliably quantify (average $\leq$100 ng/mL). However, in fractions containing older cells, ophthalmate was easily detectable and rises to a concentration of ~3,400 ng/mL of packed RBCs in cells 35 days or older. This equates to a concentration of ~12 μM in this cell population, within the range where significant inhibition of GRedoxin activity was observed. Because this population contains RBCs ranging in age from 35 up to approximately 60 days, it is likely that the ophthalmate concentration is even higher in the oldest cells within this population.

RBC Membrane Constituents

Elucidating the relationship between intracellular metabolic changes and the appearance of cell surface or mechanical changes that trigger removal of senescent RBCs by phagocytes is critical to a complete

understanding of normal RBC turnover. We found significant changes in two metabolites that may affect surface characteristics of RBCs. First, glycerophosphorylcholine (GPC) was 30-fold higher in old RBCs (Figure 7B). GPC is both a precursor of and breakdown product derived from membrane phospholipids. We also found decreased levels of several lysophospholipids and choline in older RBCs (Figure 7A). Changes in these levels may be an indication of lipid breakdown or membrane remodeling as RBCs age. Second, we found a significant decrease in the concentration of n-acetylneuraminate, also known as sialic acid, in older RBCs (Figure 7C). Sialic acid residues are components of glycoproteins, and there are several highly "sialylated" proteins on the RBC surface. Loss of cell surface sialic acid following cleavage with neuraminidase sensitizes RBC to recognition by phagocytic cells and reduces RBC survival *in vivo* (Aminoff et al., 1977).

Finally, an interesting observation was the ~10-fold decrease in ergothioneine levels (Figure 8) with increasing RBC age. Ergothioneine is a thiourea derivative of histidine produced by fungi or actinobacteria (Genghof, 1970) and derived exclusively through the diet in mammals (Melville et al., 1955). It is a xenobiotic scavenger of hydroxyl radicals and an inhibitor of iron or copper ion-dependent generation of hydroxyl radicals from H_2O_2 (Akanmu et al., 1991). Decreases in ergothioneine have been seen in redox-sensitive disease states (Chaves et al., 2019; Servillo et al., 2017); here we show that these concentrations decrease dramatically with normal RBC aging as well.

DISCUSSION

In vivo Metabolomic Profiling of RBC Survival

Utilizing a sensitive, untargeted metabolomic approach we have followed the relative concentration of small molecule metabolites in normal murine RBC as a function of cell age *in vivo* in order to identify changes that may contribute to normal cell turnover. Among the 167 metabolites identified (Table S2) and followed for changes in concentration over the course of red cell aging, the most common change in metabolite concentration observed was a steep decline when comparing the youngest cell population ($\leq$8 days) against cells $\geq$15 or 35 days. This pattern was observed for numerous metabolites including several carnitines (10), amino acids (7), and nucleotides (3). Many metabolites demonstrating this pattern of expression derive from metabolic pathways/machinery present in reticulocytes (for instance, protein synthetic pathways, mitochondrial metabolism) but are lost during maturation—explaining a steep drop in concentration when comparing a cell fraction highly enriched in reticulocytes (up to 25% reticulocytes in cells $\leq$8 days) against older cells (devoid of reticulocytes). There were several additional compounds that showed a continuing decline in concentration with increasing cell age, including additional amino acids (8), spermidine, uridine, betaine, fructose, fructose 6P, mannose 6P, N-acetylneuraminate, gulono-1,4-lactone, and pyruvate. Very few metabolites showed a consistent pattern of increase as a function of time during RBC aging. The two most prominent examples of metabolites showing an increase, glycerophosphocholine and ophthalmate, are considered in more detail below.

Metabolic Alterations of the Glycolytic Pathway

We found evidence for impaired glucose utilization in older RBCs including increased glucose (~3 fold) and decreased glucose-6-P and fructose-6-P, a combination of changes that indicate older cells have reduced hexokinase activity. Direct assay of hexokinase activity in young versus old RBC confirmed a drop in activity with increasing cell age. However, this drop was most pronounced when comparing the youngest RBC ($\leq$ 8 days) against either $\geq$15- or $\geq$35-day-old RBC (Figure 4B), whereas the change in glucose utilization was observed only in the oldest RBC population. In parallel, we measured ATP levels in young and old RBCs and found that ATP levels were consistently lower in older RBCs (Figure 4D). Because ATP is a required cofactor for hexokinase, these data imply that a combination of lower enzyme activity and lower ATP levels impact glucose utilization in older RBCs. Impaired glucose utilization in older cells will result in decreased ATP production through the glycolytic pathway and decreased NADPH production through the hexose monophosphate shunt. Interestingly, we found that G6PD exhibited a progressive time-dependent decay in activity (Figure 4C), potentially further limiting NADPH production in older cells. Both ATP and NADPH are critical for maintaining RBC homeostasis in part through maintenance of electrolyte gradients and reduction of oxidative damage.

Disruptions in Glutathione Synthesis and Utilization Pathways

The pattern of change in glutathione-related metabolites presented a more complex picture. Contrary to our expectation, we did not find lower GSH or increased GSSG levels when comparing RBCs of different

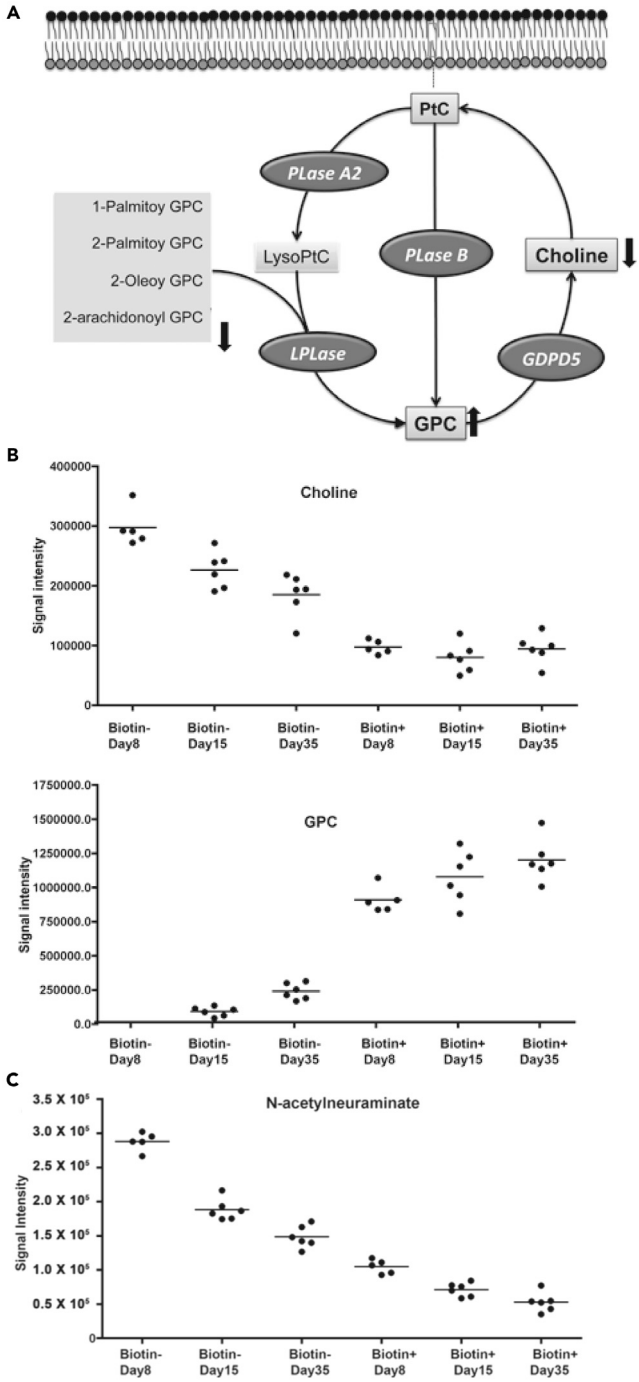

Figure 7. Changes in Glycerophosphocholine and Related Metabolites During RBC Aging

(A) Schematic of phospholipid metabolism showing the relationship between GPC, choline, and GPC-containing lysophospholipids. The decreased concentration of several lysophospholipids with increasing RBC age may indicate lipid breakdown resulting in increased GPC levels.

(B) Relative metabolite concentrations for choline and GPC are divergent over the course of RBC aging. The concentration of GPC is below the level of detection in the youngest RBC and rises progressively with increasing cell age. Choline levels remain low in older RBC, despite progressive increase in GPC. This may indicate a block in conversion of GPC to choline in older cells.

(C) Sialic acid (N-acetylneuraminate), a sugar residue found in glycoproteins, shows a progressive decline with increasing RBC age. Horizontal bars reflect the mean measurements for each corresponding condition.

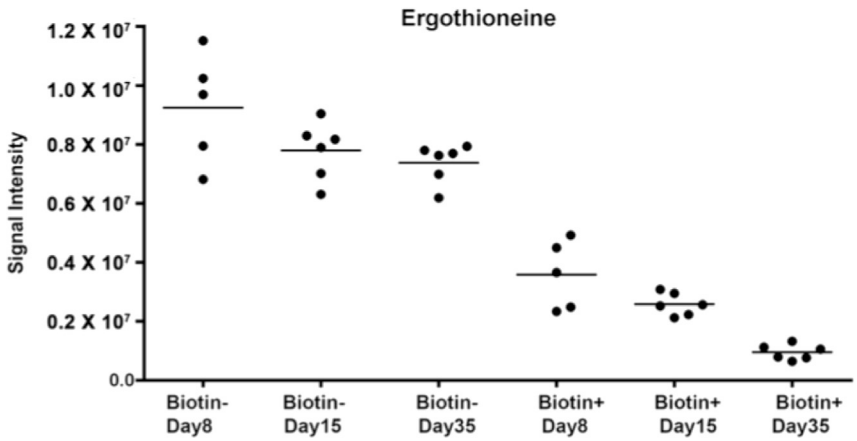

Figure 8. Ergothioneine Concentration During RBC Aging

Ergothioneine, a xenobiotic with putative antioxidant properties, is highest in the youngest RBCs and shows a progressive decline with increasing RBC age. Horizontal bars reflect the mean measurements for each corresponding condition.

age. However, changes in concentration of several precursors, breakdown products and GSH-related metabolites indicate that GSH synthesis and utilization change significantly as a function of RBC age. The most salient example of this age-dependent change was an accumulation of ophthalmate (Waley, 1958) with increasing RBC age (Figures 5 and 6). Ophthalmate is a GSH analog produced by the same synthetic pathway as GSH, with substitution of 2-aminobutyrate in place of cysteine. Ophthalmate synthesis has been reported to increase in the context of oxidative stress and cysteine depletion (Kombu et al., 2009; Soga et al., 2006) in the liver and recently measured in aging human RBC (Chaleckis et al., 2016). The time-dependent increase in ophthalmate observed during RBC aging suggests that cysteine becomes limiting and that oxidative stress increases as cells age. Although cysteine was not detected in RBC in this experiment, evidence for limited cysteine comes from the observed decrease with RBC age in cysteinyl-glycine and cysteine-glutathione disulfide (Figure 5B). In a second set of metabolomic analyses we were able to detect cysteine in biotin(−) RBC fractions (containing younger cells) but not in biotin(+) fractions, confirming loss of cysteine with increasing RBC age (data not shown).

A unifying hypothesis accounting for a GSH precursor (cysteine) limitation but consistent with our measured relative GSH and GSSG concentrations during RBC aging is that both GSH synthesis and GSH utilization are reduced in parallel in aged RBCs. This could be due to lower activity of key GSH utilizing enzymes in old RBCs (GST, GPx, or GRedoxin). When assayed, we found a profound age-dependent decline in GST activity and a more modest decline of GRedoxin activity in older RBC (Figure 6), indicating that GSH utilization is impaired in older RBCs. The accumulation of ophthalmate with increasing cell age presented another possibility—that GSH utilization could be progressively impaired as RBCs age by competitive inhibition with increasing concentrations of ophthalmate, a structural analog of GSH, and is also consistent with rMAR calculations (Figure 3). Increasing concentrations of ophthalmate strongly inhibited GRedoxin (Figure 6G) activity in normal, unfractionated RBC hemolysates. Importantly, significant inhibition of GRedoxin activity was observed at ophthalmate concentrations within the range (12 μmolar) present in ≥35-day RBCs as determined by absolute quantitation with a deuterated ophthalmate standard (Figure 6F). This constellation of metabolite concentration and enzymatic activity changes suggest a balanced dysfunction in older RBC, a decline in GSH synthesis and a decline in GSH utilization that allow maintenance of normal concentrations of GSH and GSSG but with reduced physiologic reserve. Importantly, GReductase activity shows only a modest decline in activity when comparing young versus old RBCs and no trend toward reduced activity with increasing RBC age (Figure 6C). Interestingly, GReductase activity shows a modest, reproducible, and dose-dependent increase in activity in the presence of ophthalmate (Figure 6D). These enzymatic activities are consistent with the observed modest increase in GSH and lack of change in GSSG concentrations observed in RBCs >35 days of age. Extrapolation of these time-dependent changes from a mixed cell population ≥35 days of age to cells at the terminus of murine RBC lifespan at ~50 days is likely to reveal even more severe limitations on GSH synthesis and utilization. One prediction of such a severe reduction in GSH availability would be the accumulation of oxidized cysteine residues in proteins with

increasing RBC age. Using a transgenic murine line expressing a redox sensitive GFP protein in RBC, we recently demonstrated a redox shift toward a more oxidized state with increasing cell age, consistent with this prediction (Xu et al., 2011). In that study, a significant redox shift first became apparent when comparing young versus old RBCs at 14 days, with the magnitude of the shift increasing up to the termination of the experiment at 49 days. Although the redox GFP sensor indicated that unreduced disulfide bonds accumulate in RBCs with age, we found no increase in protein carbonyls, another type of oxidative lesion, as RBCs aged (data not shown). This may indicate that carbonyls do not form during RBC aging, that there is a mechanism within RBC for degradation or removal of protein carbonyls, or that RBC harboring significant amounts of protein carbonyls are targeted for removal from circulation, limiting accumulation. This contrasts with the accumulation of protein carbonyls observed in the context of inherited defects in RBC antioxidant proteins such as PRDX2 (Lee et al., 2003) and SOD2 (Friedman et al., 2004).

Systemwide Alterations in Metabolism across the Entire RBC Network

Figure 3 summarizes the collective set of changes in the metabolite concentrations for the young versus old cells (8 versus 35 day), in the context of a mass balanced metabolic network as a function of rMAR (reflecting relative changes in biochemical reaction fluxes at two different states, corresponding to difference cell populations in these analyses). Focusing on the reactions involving metabolites with larger relative concentration changes (see Table S3), there were significant changes in all subsystems of RBC metabolism multiple age-limiting enzymes identified (reactions with large, red arrows in Figure 3). Although the older red cells are able to maintain their energy charge, the diversion and interruption of the biochemical transformations that maintain ATP, ADP, AMP, and phosphate balances indicate that most likely, as a result of the decreased hexokinase activity, older erythrocytes will be less tolerant of energy loads. Another dramatic change observed in the young versus old erythrocytes involved metabolism of glutathione and its constituent amino acids. Although directionality and magnitude of the changes are subject to influences by allosteric regulation and age-dependent changes in enzymatic activity, the shifts in the relative concentrations of glycine, aspartate, isoleucine, and ophthalmate are indicative of the shifts in reaction fluxes for glutathione synthesis and degradation. For example, discordant shifts in glutathione biosynthetic precursors availability (glutamine, cysteine, and glycine) that enable maintenance of the overall pool, while also diverting substrates to an alternative product, ophthalmate (essentially shunting glycine and glutamate for ophthalmate production). Interestingly, changes in the metabolites and the pathways of the network (Figure 3) for *in vivo* aging have significant overlap with metabolites that were predictive of "old" versus "fresh" blood in packed RBCs for storage *in vitro*, such as glucose, 5-oxoproline, pentose phosphate intermediates, and malate (D'Alessandro et al., 2017; Paglia et al., 2016; Yoshida et al., 2019). The relative concordance between the two may indicate that interventions for counteracting pre-mature senescence *in vivo* may also have applications for *in vitro* storage. Additionally, further investigation of storage lesions tracing levels of ophthalmate and ergothioneine may be warranted.

Age-Related Alterations in Ergothioneine and GPC

Ergothioneine (Fraser, 1951), a ubiquitous xenobiotic with putative antioxidant (Akanmu et al., 1991; Aruoma et al., 1997; Paul and Snyder, 2010) and cytoprotective properties (Paul and Snyder, 2010), showed a time-dependent decay in abundance as RBCs age (Figure 8). Although not recognized as a vitamin, this xenobiotic is actively absorbed from food and recycled through a specific membrane transporter (OCTN1) (Grundemann et al., 2005). Ergothioneine appears to have a specific function in erythroid cells as knockdown of OCTN1 in cell culture and zebrafish models interferes with erythroid development (Nakamura et al., 2007) and heme biosynthesis (Nilsson et al., 2009). Although ergothioneine is transported much more efficiently than any other OCTN1 substrate tested, it has not yet been proven to be the physiologically relevant substrate (Bacher et al., 2009). In the context of RBC aging, loss or elution of ergothioneine from RBCs is progressive with time. By analogy to the antioxidant properties of ergothioneine in cell culture, this loss may increase RBC susceptibility to oxidative damage and thus be a contributor to senescence. Because ergothioneine is exclusively derived from the diet there are likely to be wide variations in RBC ergothioneine concentrations between individuals (or animals) that are diet dependent. It will be very interesting to determine whether variations in ergothioneine concentration correlate with RBC survival or susceptibility to hemolytic insults in clinical or experimental settings. Similarly, if ergothioneine has antioxidant activity in RBC, increasing ergothioneine concentrations (potentially through dietary changes) may be beneficial in RBC disorders where oxidative damage impacts cell survival.

GPC accumulation in RBCs was the most dramatic metabolite increase we detected during RBC aging (>40-fold increase) and may indicate breakdown of phosphatidylcholine (PtC) in the RBC membrane (Selle et al., 1992,

1993). If membrane phospholipid degradation is coupled to GPC accumulation, we would expect to find some changes in GPC containing phospholipids as a function of cell age. As shown in Figure 7, there is a corresponding decline in some GPC-containing phospholipids (1- and 2- palmitoylglycerophosphocholine, 2- oleoylglycerophosphocholine, and 2-arachidonoylglycerophosphocholine) with increasing RBC age—and breakdown of these lipids could be the source of increased GPC. Choline, a downstream breakdown product of GPC, is present at lower concentration in older RBCs (Figure 7B), raising the possibility that accumulation of GPC is also affected by loss of activity of GPC:choline phosphodiesterase (GDPD5), the enzyme that hydrolyzes GPC to yield choline and glycerol-3-phosphate (Gallazzini et al., 2008; Lang et al., 2008). The ultimate fate of senescent RBCs is to be removed from circulation upon acquisition of a physical or cell surface change recognized by reticuloendothelial cells. Exposure of phosphatidyl-serine (Kuypers et al., 1996; Sambrano and Steinberg, 1995) and acquired changes in the band 3 protein (Kay, 1984; Low et al., 1985) have been identified or proposed as triggers for macrophage recognition of damaged or aged RBCs. Our metabolomic results suggest broader changes in membrane lipid metabolism occur with RBC aging, potentially generating age-dependent cell surface signals. Finally, we identified an additional age-related metabolic change that may impact the surface phenotype of RBC—a decline in N-acetylneuraminate, or sialic acid. Because previous studies treating RBC with neuraminidase have demonstrated the importance of surface sialic acid residues for RBC survival (Aminoff et al., 1977; Durocher et al., 1975), it is appealing to link our observation of declining sialic acid over time to the removal of aged RBC from the circulation. However, the source of sialic acid (membrane glycoproteins versus cytosolic pool) has yet to be determined and is an important question to address in future studies.

In summary, dynamic profiling of *in vivo* red cell metabolism during the normal life span of the cells revealed alterations that were expected (i.e., decline of glycolytic capability through loss of hexokinase activity) and also revealed alternative uses of the glutathione metabolism pathway in addition to identifying changes in cell membrane constituents, which were detected through differential metabolic pathway activity. Although metabolite coverage was extensive, not all metabolites of interest (ATP, NADPH, NADH, and cysteine for instance) were identified in RBC extracts owing to technical limitations. Detection failures may result from low quantities of the analytes in question, lack of sensitivity, or non-optimized extraction, or chromatography conditions for specific compounds. An initial range-finding study performed prior to the time course experiment found that extraction of 50 μL of packed RBCs allowed for consistent detection of the highest number of metabolites. This volume requirement placed a practical upper limit on the duration of time elapsed between RBC labeling and harvest of approximately 35 days, a time point where 10%–20% of RBCs remained biotin labeled. Similarly, collection of sufficient numbers of newly formed, unlabeled RBCs after *in vivo* biotinylation required adoption of a strategy of labeling, followed 24 h later by phlebotomy to stimulate erythropoiesis. One week later, sufficient new cells were present to facilitate metabolomic analysis. By selecting early, mid, and late time points, we have been able to identify specific metabolites that change with RBC aging and to derive information on the trajectory of the concentration change versus time. It will be of interest to push these experiments to time points even further along the RBC survival curve in the future (when technology or experimental design allows), although this initial analysis provides several insights into changes during *in vivo* RBC aging, particularly with respect to maintenance of redox states and membrane lipids, some of which may be translated into the clinic. One interesting application of these results would be the development of a test to determine average RBC age and thus estimate rates of RBC turnover in normal or pathologic settings. Potential RBC metabolic clock components for such a test would include ergothioneine, ophthalmate, and GPC. Although we have utilized an untargeted metabolomic approach to identify biochemical changes that occur during the normal physiologic process of RBC aging, we believe this approach will have broad utility as a novel probe in the evaluation of RBC pathology.

Limitations of the Study

Although we have identified a number of time-dependent changes in metabolite abundance as a function of RBC aging *in vivo*, the importance of each individual change as a potential determinant of RBC lifespan *in vivo* needs to be addressed. Similarly, in pathologic conditions where RBC lifespan is shortened, tracking of these metabolites (and perhaps additional compounds) during RBC aging is needed to identify critical changes that correlate with specific disorders.

Resource Availability

Lead Contact

Further information and requests for resources and reagents should be directed to and will be fulfilled by the Lead Contact, Jeffrey Friedman (friedmanbioventure@icloud.com).

Material Availability

Any novel reagents generated in this study will be made available on request, but we may require a payment and/or a completed Materials Transfer Agreement if there is potential for commercial application.

Data and Code Availability

The published article and supplementary files include all datasets generated or analyzed during this study. No novel code was used in our analysis.

METHODS

All methods can be found in the accompanying Transparent Methods supplemental file.

SUPPLEMENTAL INFORMATION

Supplemental Information can be found online at https://doi.org/10.1016/j.isci.2020.101630.

ACKNOWLEDGMENTS

The authors thank Jon Z. Long for support in design of the OA LC-MS analytical protocol. The authors thank Sherry Niessen and Patty Tu at The Center for Physiological Proteomics (http://www.scripps.edu/research/chemphys/center.html) for support and assistance in operating the Agilent 6410 TQMS. The authors thank Bruce Torbett for helpful discussion. Funding for this study came from NIH RO1 DK080232, R21 DK075763, and W8IXWH-10-2-0059 from the US Army (all awarded to J.S.F.). Salary support was provided by NIH NCATS KL2TR001882 to N.J.

AUTHOR CONTRIBUTIONS

J.S.F. conceived of the study and drafted the manuscript. X.X., K.v.L., and K.S. conducted the experiments. M.S. performed RBC lysis/extraction for measurement of metabolites and established quantification method for ophthalmate. R.P.M. and E.D.K. carried out metabolomics measurements at Metabolon, Inc. N.J. analyzed the metabolomic data. All authors reviewed the manuscript and agree on the final content.

DECLARATION OF INTERESTS

The authors declare no competing interests.

Received: May 15, 2020
Revised: August 4, 2020
Accepted: September 25, 2020
Published: October 23, 2020

REFERENCES

Akanmu, D., Cecchini, R., Aruoma, O.I., and Halliwell, B. (1991). The antioxidant action of ergothioneine. Arch. Biochem. Biophys. *288*, 10–16.

Aminoff, D., Bruegge, W.F., Bell, W.C., Sarpolis, K., and Williams, R. (1977). Role of sialic acid in survival of erythrocytes in the circulation: interaction of neuraminidase-treated and untreated erythrocytes with spleen and liver at the cellular level. Proc. Natl. Acad. Sci. U S A *74*, 1521–1524.

Arnold, L.W., and Haughton, G. (1992). Autoantibodies to phosphatidylcholine. The murine antibromelain RBC response. Ann. N Y Acad. Sci. *651*, 354–359.

Aruoma, O.I., Whiteman, M., England, T.G., and Halliwell, B. (1997). Antioxidant action of ergothioneine: assessment of its ability to scavenge peroxynitrite. Biochem. Biophys. Res. Commun. *231*, 389–391.

Bacher, P., Giersiefer, S., Bach, M., Fork, C., Schomig, E., and Grundemann, D. (2009). Substrate discrimination by ergothioneine transporter SLC22A4 and carnitine transporter SLC22A5: gain-of-function by interchange of selected amino acids. Biochim. Biophys. Acta *1788*, 2594–2602.

Beppu, M., Mizukami, A., Nagoya, M., and Kikugawa, K. (1990). Binding of anti-band 3 autoantibody to oxidatively damaged erythrocytes. Formation of senescent antigen on erythrocyte surface by an oxidative mechanism. J. Biol. Chem. *265*, 3226–3233.

Beutler, E., and Hartman, G. (1985). Age-related red cell enzymes in children with transient erythroblastopenia of childhood and with hemolytic anemia. Pediatr. Res. *19*, 44–47.

Bordbar, A., Jamshidi, N., and Palsson, B.O. (2011). iAB-RBC-283: a proteomically derived knowledge-base of erythrocyte metabolism that can be used to simulate its physiological and patho-physiological states. BMC Syst. Biol. *5*, 110.

Chaleckis, R., Murakami, I., Takada, J., Kondoh, H., and Yanagida, M. (2016). Individual variability in human blood metabolites identifies age-related differences. Proc. Natl. Acad. Sci. U S A *113*, 4252–4259.

Chaves, N.A., Alegria, T.G.P., Dantas, L.S., Netto, L.E.S., Miyamoto, S., Bonini Domingos, C.R., and da Silva, D.G.H. (2019). Impaired antioxidant capacity causes a disruption of metabolic homeostasis in sickle erythrocytes. Free Radic. Biol. Med. *141*, 34–46.

Clark, M.R., and Shohet, S.B. (1985). Red cell senescence. Clin. Haematol. *14*, 223–257.

Cohen, R.M., Franco, R.S., Khera, P.K., Smith, E.P., Lindsell, C.J., Ciraolo, P.J., Palascak, M.B., and Joiner, C.H. (2008). Red cell life span

heterogeneity in hematologically normal people is sufficient to alter HbA1c. Blood *112*, 4284–4291.

D'Alessandro, A., Gray, A.D., Szczepiorkowski, Z.M., Hansen, K., Herschel, L.H., and Dumont, L.J. (2017). Red blood cell metabolic responses to refrigerated storage, rejuvenation, and frozen storage. Transfusion *57*, 1019–1030.

Durocher, J.R., Payne, R.C., and Conrad, M.E. (1975). Role of sialic acid in erythrocyte survival. Blood *45*, 11–20.

Evans, A.M., DeHaven, C.D., Barrett, T., Mitchell, M., and Milgram, E. (2009). Integrated, nontargeted ultrahigh performance liquid chromatography/electrospray ionization tandem mass spectrometry platform for the identification and relative quantification of the small-molecule complement of biological systems. Anal. Chem. *81*, 6656–6667.

Foller, M., Huber, S.M., and Lang, F. (2008). Erythrocyte programmed cell death. IUBMB Life *60*, 661–668.

Fraser, R.S. (1951). Blood ergothioneine levels in disease. J. Lab. Clin. Med. *37*, 199–206.

Friedman, J.S., Lopez, M.F., Fleming, M.D., Rivera, A., Martin, F.M., Welsh, M.L., Boyd, A.S., Doctrow, S.R., and Burakoff, S.J. (2004). SOD2 deficiency anemia: protein oxidation and altered protein expression reveal targets of damage, stress response and anti-oxidant responsiveness. Blood *104*, 2565–2573.

Friedman, J.S., Rebel, V.I., Derby, R., Bell, K., Huang, T.T., Kuypers, F.A., Epstein, C.J., and Burakoff, S.J. (2001). Absence of mitochondrial superoxide dismutase results in a murine hemolytic anemia responsive to therapy with a catalytic antioxidant. J. Exp. Med. *193*, 925–934.

Gallazzini, M., Ferraris, J.D., and Burg, M.B. (2008). GDPD5 is a glycerophosphocholine phosphodiesterase that osmotically regulates the osmoprotective organic osmolyte GPC. Proc. Natl. Acad. Sci. U S A *105*, 11026–11031.

Genghof, D.S. (1970). Biosynthesis of ergothioneine and hercynine by fungi and Actinomycetales. J. Bacteriol. *103*, 475–478.

Grundemann, D., Harlfinger, S., Golz, S., Geerts, A., Lazar, A., Berkels, R., Jung, N., Rubbert, A., and Schomig, E. (2005). Discovery of the ergothioneine transporter. Proc. Natl. Acad. Sci. U S A *102*, 5256–5261.

Hoffmann-Fezer, G., Maschke, H., Zeitler, H.J., Gais, P., Heger, W., Ellwart, J., and Thierfelder, S. (1991). Direct in vivo biotinylation of erythrocytes as an assay for red cell survival studies. Ann. Hematol. *63*, 214–217.

Kay, M.M. (1984). Localization of senescent cell antigen on band 3. Proc. Natl. Acad. Sci. U S A *81*, 5753–5757.

Kay, M.M., Marchalonis, J.J., Schluter, S.F., and Bosman, G. (1991). Human erythrocyte aging: cellular and molecular biology. Transfus. Med. Rev. *5*, 173–195.

Kombu, R.S., Zhang, G.F., Abbas, R., Mieyal, J.J., Anderson, V.E., Kelleher, J.K., Sanabria, J.R., and Brunengraber, H. (2009). Dynamics of glutathione and ophthalmate traced with 2H-enriched body water in rats and humans. Am. J. Physiol. Endocrinol. Metab. *297*, E260–E269.

Kuypers, F.A., Lewis, R.A., Hua, M., Schott, M.A., Discher, D., Ernst, J.D., and Lubin, B.H. (1996). Detection of altered membrane phospholipid asymmetry in subpopulations of human red blood cells using fluorescently labeled annexin V. Blood *87*, 1179–1187.

Lang, K.S., Lang, P.A., Bauer, C., Duranton, C., Wieder, T., Huber, S.M., and Lang, F. (2005). Mechanisms of suicidal erythrocyte death. Cell Physiol. Biochem. *15*, 195–202.

Lang, Q., Zhang, H., Li, J., Yin, H., Zhang, Y., Tang, W., Wan, B., and Yu, L. (2008). Cloning and characterization of a human GDPD domain-containing protein GDPD5. Mol. Biol. Rep. *35*, 351–359.

Lee, T.H., Kim, S.U., Yu, S.L., Kim, S.H., Park do, S., Moon, H.B., Dho, S.H., Kwon, K.S., Kwon, H.J., Han, Y.H., et al. (2003). Peroxiredoxin II is essential for sustaining life span of erythrocytes in mice. Blood *101*, 5033–5038.

Low, P.S., Waugh, S.M., Zinke, K., and Drenckhahn, D. (1985). The role of hemoglobin denaturation and band 3 clustering in red blood cell aging. Science *227*, 531–533.

Melville, D.B., Horner, W.H., Otken, C.C., and Ludwig, M.L. (1955). Studies on the origin of ergothioneine in animals. J. Biol. Chem. *213*, 61–68.

Mercolino, T.J., Arnold, L.W., and Haughton, G. (1986). Phosphatidyl choline is recognized by a series of Ly-1+ murine B cell lymphomas specific for erythrocyte membranes. J. Exp. Med. *163*, 155–165.

Nakamura, T., Sugiura, S., Kobayashi, D., Yoshida, K., Yabuuchi, H., Aizawa, S., Maeda, T., and Tamai, I. (2007). Decreased proliferation and erythroid differentiation of K562 cells by siRNA-induced depression of OCTN1 (SLC22A4) transporter gene. Pharm. Res. *24*, 1628–1635.

Nilsson, R., Schultz, I.J., Pierce, E.L., Soltis, K.A., Naranuntarat, A., Ward, D.M., Baughman, J.M., Paradkar, P.N., Kingsley, P.D., Culotta, V.C., et al. (2009). Discovery of genes essential for heme biosynthesis through large-scale gene expression analysis. Cell Metab. *10*, 119–130.

Paglia, G., D'Alessandro, A., Rolfsson, O., Sigurjonsson, O.E., Bordbar, A., Palsson, S., Nemkov, T., Hansen, K.C., Gudmundsson, S., and Palsson, B.O. (2016). Biomarkers defining the metabolic age of red blood cells during cold storage. Blood *128*, 43–50.

Paul, B.D., and Snyder, S.H. (2010). The unusual amino acid L-ergothioneine is a physiologic cytoprotectant. Cell Death Differ. *17*, 1134–1140.

Rettig, M.P., Low, P.S., Gimm, J.A., Mohandas, N., Wang, J., and Christian, J.A. (1999). Evaluation of biochemical changes during in vivo erythrocyte senescence in the dog. Blood *93*, 376–384.

Sambrano, G.R., and Steinberg, D. (1995). Recognition of oxidatively damaged and apoptotic cells by an oxidized low density lipoprotein receptor on mouse peritoneal macrophages: role of membrane phosphatidylserine. Proc. Natl. Acad. Sci. U S A *92*, 1396–1400.

Selle, H., Chapman, B.E., and Kuchel, P.W. (1992). Release of choline by phospholipase D and a related phosphoric diester hydrolase in human erythrocytes. 1H spin-echo n.m.r. studies. Biochem. J. *284* (Pt 1), 61–65.

Selle, H., Chapman, B.E., and Kuchel, P.W. (1993). Glycerophosphocholine release in human erythrocytes. 1H spin-echo and 31P-NMR evidence for lysophospholipase. Eur. J. Biochem. *212*, 411–416.

Servillo, L., D'Onofrio, N., and Balestrieri, M.L. (2017). Ergothioneine antioxidant function: from chemistry to cardiovascular therapeutic potential. J. Cardiovasc. Pharmacol. *69*, 183–191.

Soga, T., Baran, R., Suematsu, M., Ueno, Y., Ikeda, S., Sakurakawa, T., Kakazu, Y., Ishikawa, T., Robert, M., Nishioka, T., et al. (2006). Differential metabolomics reveals ophthalmic acid as an oxidative stress biomarker indicating hepatic glutathione consumption. J. Biol. Chem. *281*, 16768–16776.

Thorburn, D.R., and Beutler, E. (1991). The loss of enzyme activity from erythroid cells during maturation. Adv. Exp. Med. Biol. *307*, 15–27.

van Wijk, R., and van Solinge, W.W. (2005). The energy-less red blood cell is lost: erythrocyte enzyme abnormalities of glycolysis. Blood *106*, 4034–4042.

Vaysse, J., Gattegno, L., Bladier, D., and Aminoff, D. (1986). Adhesion and erythrophagocytosis of human senescent erythrocytes by autologous monocytes and their inhibition by beta-galactosyl derivatives. Proc. Natl. Acad. Sci. U S A *83*, 1339–1343.

Waley, S.G. (1958). Acidic peptides of the lens. 3. The structure of ophthalmic acid. Biochem. J. *68*, 189–192.

Xu, X., von Lohneysen, K., Soldau, K., Noack, D., Vu, A., and Friedman, J.S. (2011). A novel approach for in vivo measurement of mouse red cell redox status. Blood *118*, 3694–3697.

Yoshida, T., Prudent, M., and D'Alessandro, A. (2019). Red blood cell storage lesion: causes and potential clinical consequences. Blood Transfus. *17*, 27–52.

Zimran, A., Torem, S., and Beutler, E. (1988). The in vivo ageing of red cell enzymes: direct evidence of biphasic decay from polycythaemic rabbits with reticulocytosis. Br. J. Haematol. *69*, 67–70.

iScience, Volume *23*

Supplemental Information

Metabolome Changes during *In Vivo* Red Cell Aging Reveal Disruption of Key Metabolic Pathways

Neema Jamshidi, Xiuling Xu, Katharina von Löhneysen, Katrin Soldau, Rob P. Mohney, Edward D. Karoly, Mike Scott, and Jeffrey S. Friedman

Transparent Methods

Animal experiments: All animal experiments were performed with C57Bl6/J male mice from The Jackson Laboratory (Bar Harbor, ME). All experimental protocols were evaluated and approved by the animal care and use committee at TSRI.

Biotin labeling and measurement of RBC survival: Biotin labeling was done using a single intravenous injection (100 ml) of sulfo-NHS-ester biotin suspended in sterile saline at a concentration of 4mg/ml (Friedman et al., 2001; Hoffmann-Fezer et al., 1991). Once labeled, RBC survival was followed at intervals by staining a small (1-5 µl) blood sample with an avidin-conjugated fluorophore and determining the fraction of labeled cells remaining by flow cytometry (FACS).

Isolation of biotinylated cells: RBC of defined age were isolated using streptavidin-magnetic beads and LD columns (Miltenyi, Auburn, CA) to pull down biotin labeled cells for comparative biochemical studies. 100 µl of streptavidin beads were added to a variable volume of saline washed, packed red cells. The volume of packed cells used ranged between 150—600 µl, depending upon the percentage of biotinylated cells in the sample. In order to increase the fraction of biotin (-) cells available at day 8, animals for this point were phlebotomized 1 day after biotin labeling to stimulate production of new cells prior to harvest at day 8. In each separation, a total of 100 µl of biotin labeled cells was targeted for purification. Cells were distributed to those analyses requiring viable cells, with the remaining cells stored at -80°C until used for metabolomics or protein/enzyme studies. Mean purity of all biotin (+) samples was 96.4% and 87% in all biotin (-) samples. Complete purification results are presented in Table S1. Purity was determined by FACS analysis following staining with a streptavidin:PE conjugate (Southern Biotech).

Red cell enzyme studies: Hexokinase (Hk), Glucose-6-phosphate dehydrogenase (G6PD), Glutathione Peroxidase (GPx) and Glutathione-s-transferase (GST) levels were assayed as described by Beutler (Beutler, 1984). Glutaredoxin (Grx) assay was based upon the method described by Mieyal (Mieyal et al., 1991a; Mieyal et al., 1991b), measuring glutathione-dependent reduction of hydroxyethyl disulfide in the presence of glutathione reductase. The principle of each assay is similar—recording changes in OD_{340} that reflect the concentration of the reduced pyridine nucleotide NADPH. Assays were performed in a 96-well plate format at 37°C in a Spectramax plate fluorimeter (Molecular Dynamics). Kinetic data was collected for 6-20 minutes (depending upon assay) and a hemoglobin determination was performed on each sample to normalize measured enzymatic activity. Ophthalmate inhibition studies utilized enzyme assays performed in parallel with increasing concentrations of ophthalmate (Bachem) as indicated in the respective figure legends. ATP concentration was measured in RBC lysate using the CellTiter-Glo assay kit (Promega; Cat#G7570) with values normalized to hemoglobin.

Metabolomic evaluation: Untargeted metabolomic profiling was performed at Metabolon (Durham, NC) using a combination of GC-MS and LC-MS as described (Evans et al., 2009; Reitman et al., 2011). Data was collected from 50 µl of purified packed RBC for each extraction. In a range finding study, use of aliquots smaller than 25 µl reduced the number of metabolites/ features identified. 6 biologic replicates were analyzed for the day 15 and day 35 time points, and 5 biologic replicates were analyzed at day 8. For each time point, data from biotin^{+} (old) and biotin^{-} (young) fractions was obtained. For each detected metabolite, the median value across all samples analyzed (N=36; comprising 34 fractions from the 3 time points and 2 unfractionated control samples) was given an arbitrary value = 1. Each individual determination was then expressed as a ratio relative to this median value, to determine fold-change in metabolite concentration.

Statistical comparisons: Metabolomic data was analyzed using a paired t test when comparing biotin^{+} and biotin^{-} fractions derived from the same animal and same time point. Welch's two-sample t test was used between non-paired sample groups, and one-way ANOVA was used to assess significance of changes in biochemical concentration over time. Statistical analyses were performed on log-transformed data (after imputation of missing values) since a test of normality showed that the log-transformed distribution was better represented by a normal distribution than when untransformed values were used (Suhre et al., 2011).

Assay for determination of absolute concentration of ophthalmate: Metabolomic extraction of RBC samples was conducted at 4°C or on ice prior to LC-MS analysis. For each sample, a 10 µl aliquot of RBCs was added to a 1.5mL polypropylene microcentrifuge tube. 10 µl of 100 µM d2-(gly)-ophthalmic acid (Bachem Americas, Torrance, CA) and 80 µl of ice cold methanol were added, followed by vortex mixing at high speed for 30 seconds to lyse the RBCs. The samples were centrifuged at 14,000 X g for 10 minutes. 80 µl of supernatant was transferred to glass autosampler microvial inserts and stored at 4°C in the autosampler tray prior to LC-MS analysis. Quantitative analysis of OA using the deuterated standard d2-OA was based on a ratio of the non-deuterated:deuterated chromatographic integrated peak areas and was performed on the Agilent 6410 Triple Quadrupole Liquid Chromatography-Mass Spectroscopy (TQMS) instrument using positive ion analysis mode. For each sample, 40 µl of methanolic lysate were injected into the TQMS instrument and EC metabolites were measured by multiple reaction monitoring (MRM) using the following transitions : 290>58 (OA), fragmentation energy = 10, and 292>58 (2-AG), fragmentation energy = 10. Chromatography was performed using the following solvents: A - acetonitrile and B – 4g/l ammonium acetate 0.4% v/v formic acid:H2O. The lysate was injected into a 5 micron particle size, 100 Å pore size, 5 cm long aminopropyl-modified Luna column (50 X 4.6 mm) from Phenomenex (Torrance, CA) and eluted with a 24 minute chromatographic run: 0-3 minutes 0% B, from 3-10 minutes 50% B to 100% B, hold at 100% B to 20 minutes, then run at 0% B until 24 minutes. A typical retention time for OA was 10.9 minutes, for glutathione, 11.2 minutes.

Network mapping and analysis: Systems analysis of the metabolic network was carried out beginning with the recently published proteome based network reconstruction of the mature human erythrocyte iAB-RBC-253 (Bordbar et al., 2011). Further content expansion was carried out, focused on glutathione synthesis and degradation reactions. These reactions included, cysteine glutathione synthesis, gamma-glutamyl-2-aminobutyrate synthetase, ophthalmate synthetase, S-Formylglutathione hydralase, S-Nitroso-glutathione synthesis, argininosuccinate lyase, aspartate transaminase, guanidinoacetate N-methyltransferase, glycine amidinotransferase, guanine deaminase, and creatine transport with literature support when available (Bastone et al., 1990; Bennett et al., 1994; Heiskanen et al., 1994; Sandmann et al., 2005; Tsuge et al., 1987).
The intersection of the metabolites in the network and experimentally measured metabolites was determined to define a context specific network with data that can be mapped to the network. This resulted in reduction of the network from 422 metabolites (including intracellular as well as extracellular metabolites) and 562 reactions (including intracellular, transport, and exchange reactions) to 97 metabolites and 199 reactions. The reduced, metabolome-specific network was analyzed using flux balance analysis to ensure that mass conservation constraints were satisfied (Palsson, 2006). The network was used for comparison between red cell metabolome fractions of different ages, focusing on the difference between the youngest and oldest cell fractions (i.e. 8 day versus 35 day old cells). According to the Law of Mass Action, net biochemical rate equations can be expressed as the difference between the forward and reverse reaction rates,

(1) $$v = v^+ - v^-$$

Such that,

(2) $$v = v^+\left(1 - \Gamma/_{K_{eq}}\right)$$

n which v+ is the forward reaction rate, v- is the reverse reaction rate, Γ is the mass action ratio, and K_{eq} is the equilibrium constant, with $K_{eq} = k^+/k^-$ (for forward and reverse rate constants, k^+ and k^-, respectively). Based on changes in the mass action ratio, the relative Mass Action Ratio (rMAR) can be calculated for the complement of metabolites that were measured for the reactions in the network. Let $\beta = 1 - v/v^+$, so that rearrangement of equation (2) yields,

(3) $$\beta = \Gamma/_{\square_{eq}}$$

In the limiting cases, a) at equilibrium $v^+ = v^-$ then $\beta = 1$, b) when $v^- = 0$, then $\beta = 0$, c) when $v^+ > v^-$ then $\beta < 1$ and the reaction progresses in the forward direction, and d) when $v^+ < v^-$ then $\beta > 1$ and the reaction proceeds in the reverse direction (see Supplemental Information for additional details).
Although the calculated quantities cannot provide quantitative statements about flux magnitudes, ratios of the mass action ratios can provide information about changes in the thermodynamic driving potential between different conditions (or over time). It immediately follows from equations (2) and (3), for two time points, t1 and t2, corresponding to two different non-equilibrium, homeostatic states, yields,

(4) $$\Gamma_{t1}/_{\Gamma_{t2}} = \beta_{t1}/_{\beta_{t2}}$$

Ratios of Γ at two different steady states defines the rMAR, $\gamma_{t1\text{-}t2} = \Gamma_{t1}/\Gamma_{t2}$. For $\gamma_{t1\text{-}t2} >= 1$ the thermodynamic driving potential relative to t1 is shifted in the forward direction and for $\gamma_{t1\text{-}t2} < 1$, the thermodynamic driving potential at t2 relative to t1 is shifted in the reverse direction.
rMARs for the 8 day old versus 35 day old RBC are highlighted in Figure 3 (see Figure S2 for higher resolution, detailed, labeled version). The rMARs for young vs old cells for the full set of reactions, for which at least one metabolite has been measured, are listed in Table S3. This list of altered rMARs was further stratified by identifying the set of reactions that involved a metabolite whose relative concentration changes exceeded one standard deviation of the mean relative concentration changes for the mapped metabolites (see Table S3).
The change in the chemical potential (altered concentrations of metabolites) may be due to a change in the environment via altered metabolite availability, drug treatment, or change in the enzyme rate constant (through degradation, oxidation, etc). This experimental design profiles normal RBC over time, thus the former two possibilities are excluded, thus the altered metabolite ratios resulting in the changes in thermodynamic driving forces likely result from a kinetic limitation of the enzyme, or 'age-dependent limitation'.

Resource Availability

This study did not generate new, unique reagents. Further information and requests for resources and reagents should be directed to the Lead Contact, Jeffrey Friedman (friedmanbioventure@icloud.com).
Data and code availability: The published article includes all of the data generated or analyzed during this study.

Relative Mass Action Ratio:

Consider mass action kinetics with forward rate, v^+, equilibrium constant, K_{eq}, and mass action ratio, Γ,

(1) $$v = v^+(1 - \frac{\Gamma}{K_{eq}})$$

for which, by definition, $K_{eq} = k^+/k^-$ (for forward and reverse rate constants, k^+ and k^- respectively), and $\Gamma < K_{eq} \Rightarrow v > 0$. Let $\beta = 1 - v/v^+$ (from which it follows that $\beta = 1 - (1 - \Gamma/K_{eq})$, so that,

(2) $$\beta = \frac{\Gamma}{K_{eq}}$$

Such that $\beta \in [0, \infty)$. We consider the cases,

1. As β approaches $0 \Rightarrow v^-$ approaches 0 and $v = v^+$
2. $\beta = 1 \Rightarrow v = 0$ and the reaction is at equilibrium
3. $\beta < 1 \Rightarrow v^+ > v^-$ and the reaction proceeds in the forward direction
4. $\beta > 1 \Rightarrow v^+ < v^-$ and the reaction proceeds in the reverse direction

If we then consider a *ratio* of mass action ratios between to time points, the relative Mass Action Ratio (rMAR), $\gamma_{t1-t2} = \Gamma_{t1} / \Gamma_{t2}$,

(3) $$\frac{\Gamma_{t1}}{\Gamma_{t2}} = \frac{1 - {v_{t1}}/{v_{t1}^+}}{1 - {v_{t2}}/{v_{t2}^+}} = \frac{\beta_{t1}}{\beta_{t2}}$$

Evaluation of different conditions at t_1 and t_2,

1. $\beta_{t1} < 1$ and $\beta_{t2} \ll 1$ results in $\gamma_{t1/t2} > 1$ and the reaction progresses in the forward direction, but with a greater magnitude at t2.

2. $\beta_{t1} > 1$ and $\beta_{t2} < 1$ results in $\gamma_{t1/t2} > 1$ and the reaction progresses in the reverse direction at t_1, but then reverses to a forward direction at t2.

3. $\beta_{t1} > 1$ and $\beta_{t2} \gg 1$ results in $\gamma_{t1/t2} < 1$ and the reaction progresses in the reverse direction at t_1 and then increases in magnitude (further reversed) at t2,

4. $\beta_{t1} < 1$ and $\beta_{t2} > 1$ results in $\gamma_{t1/t2} < 1$ and the reaction progresses in the forward direction at t_1 and then in the reverse direction at t2.

The above four scenarious can be summarized in terms of the relative thermodynamic driving potential at t2 vs t2, so that Cases 1 and 2 are grouped together and Cases 3 and 4 are grouped together so that for $\gamma_{t1/t2}$,

1. $\gamma \geq 1 \Rightarrow$ the thermodynamic driving potential increases in the forward direction at t_2
2. $\gamma < 1 \Rightarrow$ the thermodynamic driving potential increases in the reverse direction at t_2

Supplemental Tables and Figures

Table S1 Related to Figure 2 and Table 1. Results of Purification of Biotin+ and Biotin- RBC

Day post labeling	Animal number	Biotin +	Biotin -	start Biotin +
	1	95.5	93	
	2	96.3	81	
	3	94.5	90.2	
	4	97.2	92.7	
	5			
8	6			
	1	99.4	61.8	45.2
	2	99.1	75.1	38.5
	3	99.3	75.1	45
	4	97.4	75.3	54.1
	5	98.8	82.4	40.9
15	6	98.1	89.5	36
	1	94.9	96.8	16.4
	2	90.5	98.1	14.5
	3	96.4	91.7	25.4
	4	90.5	93.8	27.3
	5	97.3	95.8	22.2
35	6	97.8	94.4	26

For the day 8 time point listed, we did not collect the pre-purification data on biotin(+) vs biotin(-). However, from multiple concurrent experiments (such as those contributing to Figure 1), the percent biotin(+) cells 8 days post-labeling ranges between 63-76%.

Table S2 Related to Figure 3. Complete list of identified metabolites and concentrations versus time (separate Excel file).

Table S3 Related to Figure S2 and Figure 3. List of metabolite abbreviations and rMAR changes (separate Excel file).

Figure S1 Related to Figure 2 and Table 1. Representative Examples of Metabolite Profiles. Panels A-D show a decline in multiple carnitine-related metabolites during RBC aging. Panels E-H show profiles for several amino acids. Most amino acids decline over the course of RBC aging, but there were exceptions such as glutamine (G). Panels H-K show a variety of patterns observed, including metabolites with little change over the time course, and those with no clear trajectory of change over time.

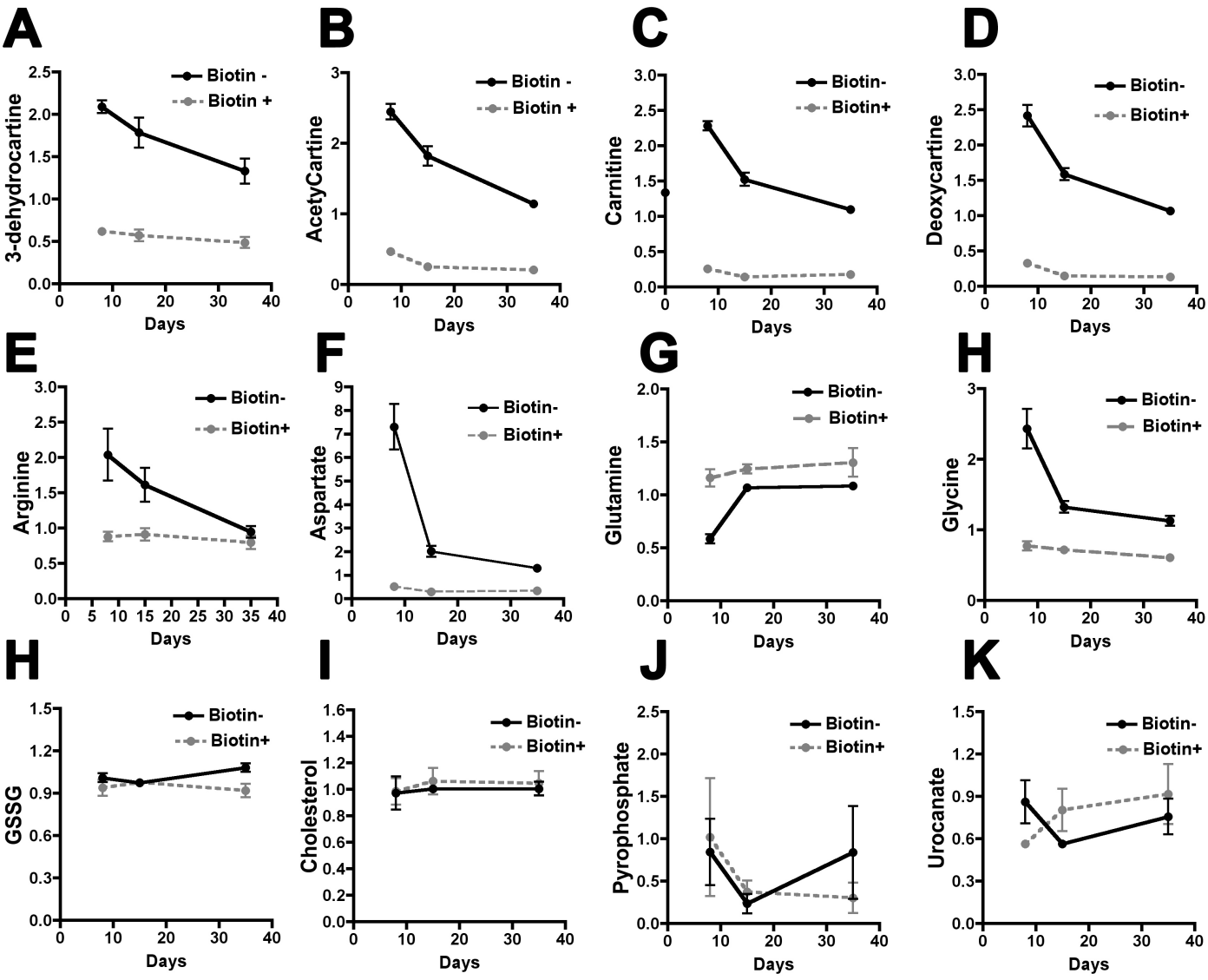

Figure S2 Related to Figure 3. Detailed annotated map of RBC metabolism MAR ratios corresponding to Figure 3 in the main text. This is a custom map of iAB-RBC-283 that has been expanded in the areas of glutathione and amino acid metabolism and curtailed in regions without experimental metabolomic measurements. The color scale and width of the reaction arrows reflect alterations in the relative Mass Action Ratios (rMAR) for the young (day 8) versus old (day 35) cells.

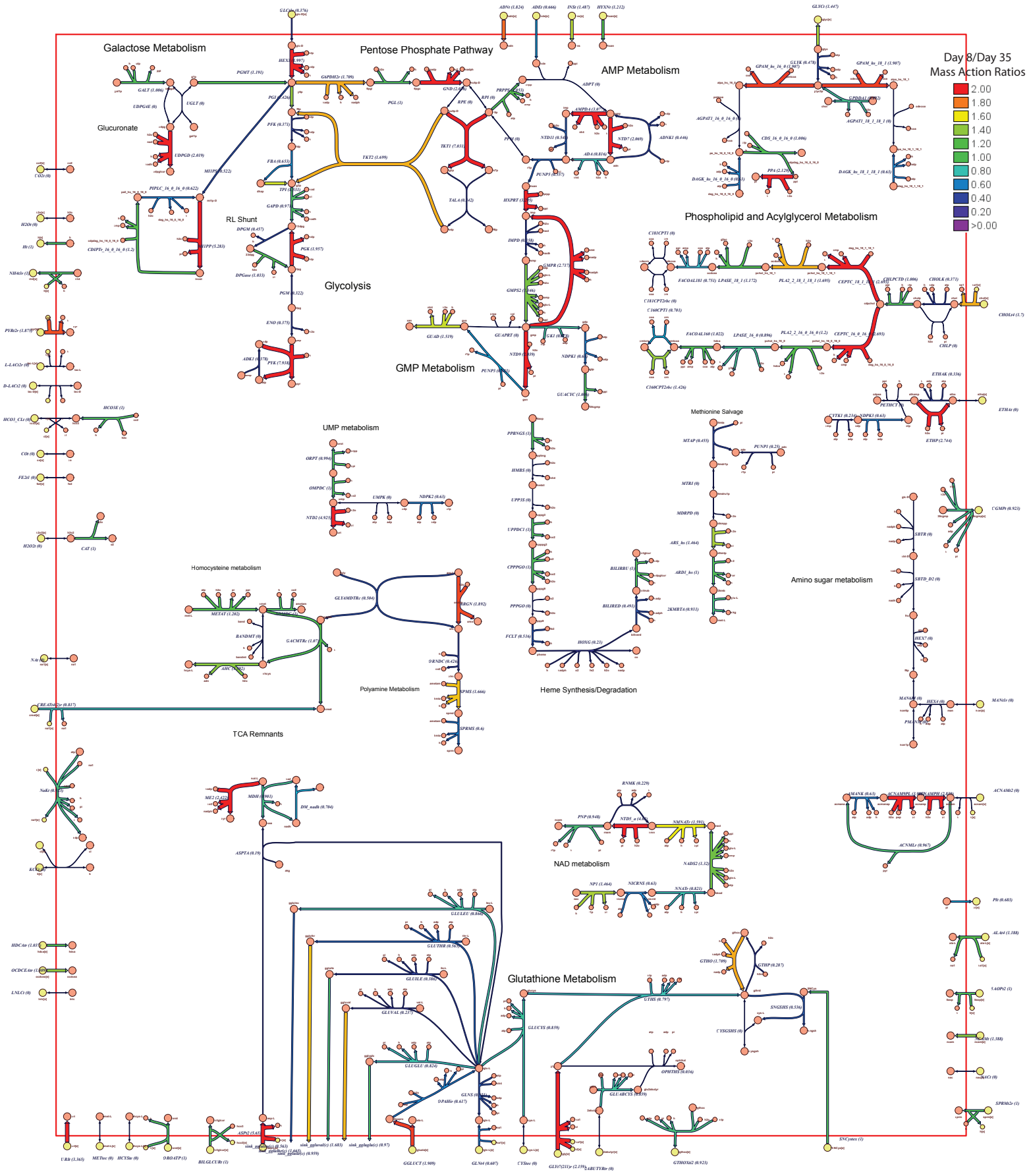
Galactose Metabolism
Pentose Phosphate Pathway
AMP Metabolism
Glucuronate
RL Shunt
Glycolysis
Phospholipid and Acylglycerol Metabolism
GMP Metabolism
UMP metabolism
Methionine Salvage
Homocysteine metabolism
Polyamine Metabolism
Heme Synthesis/Degradation
Amino sugar metabolism
TCA Remnants
NAD metabolism
Glutathione Metabolism
Day 8/Day 35
Mass Action Ratios
2.00
1.80
1.60
1.40
1.20
1.00
0.80
0.60
0.40
0.20
>0.00

References

Bastone, A., Diomede, L., Parini, R., Carnevale, F., and Salmona, M. (1990). Determination of argininosuccinate lyase and arginase activities with an amino acid analyzer. Anal Biochem *191*, 384-389.

Bennett, S.E., Bevington, A., and Walls, J. (1994). Regulation of intracellular creatine in erythrocytes and myoblasts: influence of uraemia and inhibition of Na,K-ATPase. Cell Biochem Funct *12*, 99-106.

Beutler, E. (1984). Red Cell Metabolism: A Manual of Biochemical Methods (New York, NY: Grune & Stratton, Inc.).

Bordbar, A., Jamshidi, N., and Palsson, B.O. (2011). iAB-RBC-283: A proteomically derived knowledge-base of erythrocyte metabolism that can be used to simulate its physiological and patho-physiological states. BMC Syst Biol *5*, 110.

Evans, A.M., DeHaven, C.D., Barrett, T., Mitchell, M., and Milgram, E. (2009). Integrated, nontargeted ultrahigh performance liquid chromatography/electrospray ionization tandem mass spectrometry platform for the identification and relative quantification of the small-molecule complement of biological systems. Anal Chem *81*, 6656-6667.

Friedman, J.S., Rebel, V.I., Derby, R., Bell, K., Huang, T.T., Kuypers, F.A., Epstein, C.J., and Burakoff, S.J. (2001). Absence of mitochondrial superoxide dismutase results in a murine hemolytic anemia responsive to therapy with a catalytic antioxidant. J Exp Med *193*, 925-934.

Heiskanen, K., Siimes, M.A., Perheentupa, J., and Salmenpera, L. (1994). Reference ranges for erythrocyte pyridoxal 5'-phosphate concentration and the erythrocyte aspartate transaminase stimulation test in lactating mothers and their infants. Am J Clin Nutr *59*, 1297-1303.

Hoffmann-Fezer, G., Maschke, H., Zeitler, H.J., Gais, P., Heger, W., Ellwart, J., and Thierfelder, S. (1991). Direct in vivo biotinylation of erythrocytes as an assay for red cell survival studies. Ann Hematol *63*, 214-217.

Mieyal, J.J., Starke, D.W., Gravina, S.A., Dothey, C., and Chung, J.S. (1991a). Thioltransferase in human red blood cells: purification and properties. Biochemistry *30*, 6088-6097.

Mieyal, J.J., Starke, D.W., Gravina, S.A., and Hocevar, B.A. (1991b). Thioltransferase in human red blood cells: kinetics and equilibrium. Biochemistry *30*, 8883-8891.

Palsson, B.O. (2006). Systems Biology: Determining the Capabilities of Reconstructed Networks (Cambridge, UK: Cambridge University Press).

Reitman, Z.J., Jin, G., Karoly, E.D., Spasojevic, I., Yang, J., Kinzler, K.W., He, Y., Bigner, D.D., Vogelstein, B., and Yan, H. (2011). Profiling the effects of isocitrate dehydrogenase 1 and 2 mutations on the cellular metabolome. Proc Natl Acad Sci U S A *108*, 3270-3275.

Sandmann, J., Schwedhelm, K.S., and Tsikas, D. (2005). Specific transport of S-nitrosocysteine in human red blood cells: Implications for formation of S-nitrosothiols and transport of NO bioactivity within the vasculature. FEBS Lett *579*, 4119-4124.

Suhre, K., Shin, S.Y., Petersen, A.K., Mohney, R.P., Meredith, D., Wagele, B., Altmaier, E., Deloukas, P., Erdmann, J., Grundberg, E.*, et al.* (2011). Human metabolic individuality in biomedical and pharmaceutical research. Nature *477*, 54-60.

Tsuge, A., Uchida, H., and Ishimoto, G. (1987). Erythrocyte S-formylglutathione hydrolase polymorphism in Japanese and the relation to erythrocyte esterase D polymorphism. Nihon Hoigaku Zasshi *41*, 93-96.